

FEATURE ARTICLE

Molecular Dynamics of Water at the Protein–Solvent Interface

Anna Rita Bizzarri* and Salvatore Cannistraro

*Unita' INFM, Dipartimento di Scienze Ambientali, Universita' della Tuscia, I-01100 Viterbo, Italy**Received: January 14, 2002; In Final Form: April 11, 2002*

The use of molecular dynamics simulation to investigate the properties of hydration water around proteins is outlined. A variety of structural and dynamical properties of the protein hydration water are reviewed and compared with those of bulk and with the corresponding experimental results. In particular, the accessibility to the protein medium, the hydrogen bond networking capability, the residence times, the diffusive mobility, the relaxation behavior, and the inelastic vibrational features of hydration water are analyzed in framework of the peculiar interactions of water at the protein surface. All these features, which can be traced back to the complexity of the overall protein–solvent energy landscape, are discussed in connection with the role played by hydration water in the biological functionality.

1. Introduction

Water plays a crucial role in determining the structure and the dynamics, and then the functionality, of globular proteins.^{1,2} Conversely, there is a variety of experimental^{3–15} and theoretical^{16–21} studies demonstrating that a protein in an aqueous solution modifies both the structural organization and dynamical behavior of its neighboring water layers.

Water molecules in protein solutions may be broadly classified into three categories:²² (i) strongly bound internal water, (ii) water molecules that interact with the protein surface, (iii) bulk water. Bound water molecules occupying internal cavities and deep clefts can be identified crystallographically. Such water molecules, which are extensively involved in the protein–solvent H-bonding, may play a structural role. Surface water, usually called hydration water, exhibits a heterogeneous dynamical behavior due to both the interaction with the solvent-exposed protein atoms with different chemical character and the topological disorder, or roughness, of the protein surface. Finally, water which is not in direct contact with the protein, continuously exchanging with surface water, reveals properties that approach those of bulk water as far as solvent molecules at an increasing distance from the protein surface are taken into account.

It is now well-ascertained that a threshold level of hydration (less than 0.40 grams of water per gram of protein) is required to fully activate the dynamics and functionality of globular proteins:^{23–25} such an amount being less than sufficient to completely cover the protein surface. However, a satisfactorily description of the mechanisms connecting the hydration water dynamics with those of protein is still far from being achieved. On the other hand, a deeper understanding of the dynamical coupling between the protein and the solvent, which indeed draws more and more attention of the researchers in the field, could be of extreme relevance to elucidate the enzymatic activity, the molecular recognition, and the folding process.

Proteins are complex systems, their motions causing a huge amount of different conformational substates (CS), which are

thermally activated and related to local minima of the potential energy surface.^{26–28} Actually, protein energy landscapes, very similar to those of disordered media, such as glasses,^{29,30} are characterized by the existence of many, nearly isoenergetic, local minima which are likely organized in a hierarchical way.³¹ At room temperature, fluctuations among CS occur continuously and are crucial in determining the macromolecule biological function.³¹ The solvent could be a dominant factor in the activation of these fluctuations. It has indeed been suggested that the multiplicity of water states, characterized by a different number of H-bonds and rearranging continuously,³² could be at the origin of the conformational transitions of the biomolecule.⁶ In other words, water injects fast conformational fluctuations into the protein through the continuous forming and breaking of hydrogen bonds involving the long flexible lateral chains, well-suited to adapt to the many possible water patterns.^{33–35}

When the temperature is lowered, transitions among CS can be suppressed³⁶ and the biological functionality inhibited:^{26,27} with these transitions being, on one hand, suppressed also by dehydration.³⁷ Below about 200 K, the protein becomes frozen in a kinetically arrested metastable state in analogy with what occurs in a glassy system.^{38,39} This so-called glass-like transition, verified by a variety of experimental techniques^{40–43} and of MD simulation approaches,^{44–47} is manifested by a reduction in the magnitude and an increase in the time scale of atomic fluctuations. Accordingly, the mean square displacement (MSD) of the protein atoms switches from a highly anharmonic to an essential harmonic behavior, below the transition temperature. The path to this transition was found to be highly dependent on, or “slaved” to, the solvent properties (chemical composition, viscosity, dielectric properties, etc.)^{40,48,49} Notably, the onset of the protein motions above 200 K was suggested to be triggered by the dynamics of the hydrogen bond network at the protein–solvent interface.⁵⁰ A further support to such a hypothesis comes from a recent MD simulation study which demonstrated that

the magnitudes of protein fluctuations above 200 K are drastically reduced if only the solvent temperature is kept below the glass transition temperature.⁵¹ Indeed, a more recent perceptive view indicates the dynamics of the methyl side chains as a probe of the role of water into the activation of the protein dynamical transition.⁵²

On the other hand, hydration water in the vicinity of protein surface exhibits an amorphous character, which is closely reminiscent of that of supercooled bulk water.^{1,35,53–55} Indeed, the presence of the protein can prevent solvent water at the interface from crystallization even below 60 °C.^{6,56} This aspect is of some relevance for the preservation of the functionality at low hydration conditions as well as for the freeze resistance¹ and might be also related to the drastic changes in the protein dynamics and functionality as obtained by the addition of glass-forming liquids (glycerol, trehalose etc.)^{57–59} Furthermore, it is worth of note that both protein and the surrounding hydration water relaxations were analyzed in the framework of the Mode Coupling Theory (MCT),^{40,54,60} a well-suited approach to describe the dynamics of glasses.^{35,61} Generally, the amorphous character of hydration water and the glassy behavior of proteins is an intriguing coincidence that could be accidental or may point toward a peculiar physical significance which deserves further investigation.

Protein and hydration water show the presence of an excess of low-frequency vibrational modes, over the estimated Debye level.^{62,63} The origin of such a vibrational anomaly, usually called boson peak, and representing a sort of signature of the disordered, amorphous state, is still amply debated.^{38,64,65} Indeed, the occurrence of the boson peak in several proteins characterized by a different structure^{37,66–68} and in the surrounding solvent^{62,69} led, once again, to speculate about a possible vibrational coupling between the biomolecule and the surrounding solvent; coupling of possible relevance for the biological functionality.^{62,69} Such a speculation received some ground from the observation of $1/f^\alpha$, or flickering, noise in the potential energy fluctuations of both the protein macromolecule and the surrounding solvent.⁷⁰ $1/f^\alpha$ noise, which is a manifestation, in the temporal domain, of the complexity of the system, could be, in some way, connected to the vibrational density of states and to the exploration of the complex energy landscape.^{71,72} Moreover, the fact that the exponent α was found to be the same for both the protein and its hydration water points toward an intimate relationship between the energy landscape of two systems.

In this paper, we present an overview of the dynamical properties of hydration water around proteins as investigated by MD simulation. We note in passing that MD simulation, providing a detailed atomic description of both the protein and the solvent in a temporal window ranging from femto- to nanoseconds, offers a unique opportunity to focus the attention, at the same time, on both the local and the global properties of hydration water also in relationship to the protein dynamics. A variety of aspects of hydration water dynamics are reviewed in a tight connection with the protein dynamics and functionality also focusing onto the dynamical coupling between the protein and the solvent. The crucial role played by the solvent in determining the protein dynamical behavior and, more notably, in controlling the biological function of the protein macromolecule is emphasized and discussed also in connection with the global peculiar properties of hydration water and compared with the available experimental results.

The paper is organized as follows. Section 2 briefly describes MD simulation methods applied to protein systems. In section

3, the different methods and the main results related to the structural and the dynamical properties of hydration water at the protein–solvent interface are reviewed and discussed also in connection with the protein dynamics and functionality. In particular, after a brief introduction (section 3.1), the concept of solvent accessible surface is reviewed (section 3.2). Then, the radial distribution functions of water and the concept of hydration sites at the protein surface are presented (section 3.3). Section 3.4 describes the structural and the dynamical organization of the H-bonds formed between the protein and the solvent and their implications in the dynamical properties of proteins. In section 3.5, the residence times and the relaxation decay of the survival probability function of hydration water are reviewed and discussed also in connection with the amorphous character of water around proteins. An analysis about the diffusion coefficient of hydration water at various distances from the protein surface is given in section 3.6. Section 3.7 provides an overview of the occurrence of anomalous diffusion for water moving close to the protein surface. A description of such a phenomenon in terms of a spatial or temporal disorder at the protein–solvent interface is also presented. The rotational dynamics of hydration water is given in section 3.8. Sections 3.9 and 3.10 show some MD calculated quantities which can be directly compared with neutron scattering data. In particular, the dynamical structural function, the dynamical susceptibility, the density of states and the intermediate scattering function of protein hydration water, revealing properties closely reminiscent of those of amorphous systems, are discussed. The occurrence of $1/f^\alpha$ noise in the potential energy of hydration water is discussed in section 3.11. Finally, a brief discussion and a future outlook are presented in section 4.

2. Molecular Dynamics Simulation Methods of Hydrated Protein Systems

MD simulation involves the computation of the coordinates and velocities of the system atoms as a function of time. The essential prerequisites to perform a simulation are the knowledge of a starting set of atomic coordinates and of the interaction potential between atoms. In the classical approach, Newton's law is usually used to describe the motion of individual particles, while the interaction potential is represented by an empirical energy function that takes into account for both the bonding and the nonbonding contributions:^{73–76}

$$U(\mathbf{R}) = \frac{1}{2} \sum_{\text{bonds}} K_b (b - b_0)^2 + \frac{1}{2} \sum_{\text{angle}} K_\theta (\theta - \theta_0)^2 + \frac{1}{2} \sum_{\text{dihedrals}} K_\chi [1 + \cos(n\chi - \delta)] + \frac{1}{2} \sum_{\text{impropers}} K_{\text{imp}} (\phi - \phi_0)^2 + \sum_{\text{nonbondedpairs}} \epsilon_{ij} \left[\left(\frac{\sigma_{ij}}{r_{ij}} \right)^{12} - \left(\frac{\sigma_{ij}}{r_{ij}} \right)^6 \right] + \frac{q_i q_j}{4\pi\epsilon_0 r_{ij}} \quad (1)$$

where \mathbf{R} is the coordinates of the atoms; K_b , K_θ , K_χ , and K_{imp} are the bond, angle, dihedral angle, and improper dihedral angle force constants, respectively; b , θ , χ , and ϕ are the bond length, bond angle, dihedral angle, and improper torsion angle, respectively; the subscript zero represents the equilibrium values for the individual terms. Lennard–Jones 6–12 and Coulomb terms contribute to the external or nonbonded interactions; ϵ_{ij} is the Lennard–Jones well depth, and σ_{ij} is the distance at the Lennard–Jones minimum between atoms i and j ; q_i is the partial atomic charge, ϵ_0 is the dielectric constant, and r_{ij} is the distance between atoms i and j . Different sets of parameters for empirical

potential energy function were developed (CHARMM, GRO-MOS, AMBER, and ENCAD).^{77–80} The parameters that appear in eq 1 are initially obtained from experimental and quantum mechanic studies of small molecules and then refined to yield correct experimental structural and spectroscopic results.^{77–80} The hydrogen atoms can be treated by two different approaches: the “united atom” (UA) scheme which describes non polar hydrogens as united groups (i.e., CH, CH₂, CH₃); the “all hydrogens” (AH) scheme which explicitly treats all polar and nonpolar hydrogens.

To save computational time, a variety of approximate methods for the treatment of electrostatic long range interactions were developed.⁸¹ For example, the calculation of electrostatic interactions are spherically cut at a certain distance with a possible introduction of a switching function to smoothly approach to zero. Such approximate methods, while offering simple and computationally cheap simulations, may produce some artifacts.⁸¹ Recently, the Ewald summation technique, representing a well-established method for a rigorous treatment of electrostatic interactions in periodic systems, was applied to the MD simulations of proteins;^{82–84} however, possible artifacts resulting from the introduction of artificial periodicity can be observed.⁸⁵

Equation 1 can include solvation effects in two different ways. By implicit solvation model in which the interaction parameters are modified in an attempt to make a solvated-averaged potential of mean force.^{86,87} More accurate, but also more demanding of computer resources, is the explicit incorporation of solvent molecules in the basic model.¹⁸ The water molecules are then treated on the same level as groups within the protein and are represented by additional terms in eq 1. Such an approach requires a solvent–solvent potential sufficiently accurate to describe the major physical properties of the solvent (such as the radial distribution functions, self-diffusion coefficient, density, viscosity, etc.) and a method to determine an effective solute–solvent potential, given the individual solvent–solvent and solute–solvent parameters.

A variety of potential functions to describe intermolecular liquid water interactions were proposed and tested: for example, SPC,⁸⁸ SPC/E,⁸⁹ TIP3P, TIP2, TIP4P,⁹⁰ TIP3S, F3C,⁹¹ and ST2;⁹² these models differ regarding the number of interactions sites, the geometric arrangements, and the parametrization of the charged sites. As an example, SPC and TIP3 models, commonly used in the MD simulations of hydrated protein systems, involve a rigid water monomer that is represented by three interaction sites, while the ST2 and TIP4 require four sites. The reproduction of the experimental values for some properties (e.g., density, compressibilities, diffusion coefficient, specific heat, etc.) can be assumed as validating tests for the used water models.

The water–water intermolecular potential can be generally described by the

electrostatic and the van der Waals interaction:

$$U(\mathbf{R}) = \frac{q_i q_j}{4\pi\epsilon_0 r_{ij}} + \sum_{ij} \epsilon_{ij} \left(\frac{\sigma_{ij}}{r_{ij}} \right)^{12} - \left(\frac{\sigma_{ij}}{r_{ij}} \right)^6 \quad (2)$$

where q_i is the charge of the site i , and r_{ij} is the distance between atoms i and j ; ϵ_0 is the dielectric constant; ϵ_{ij} and σ_{ij} are the Lennards–Jones parameters.

The geometries and the parameters for the water potential mostly used in the MD simulation of protein systems (SPC, SPC/E, and TIP3P) are summarized in ref 90.

The solute–solvent interaction parameters can be derived from those of the protein–protein and the solvent–solvent by applying combination rules for the Lennard–Jones parameters. Possible expressions are^{77–79}

$$\epsilon_{sp} = (\epsilon_{pp}\epsilon_{ss})^{1/2}; \sigma_{sp} = \frac{\sigma_{pp} + \sigma_{ss}}{2} \quad (3)$$

or (ref 93):

$$\epsilon_{sp} = (\epsilon_{pp}\epsilon_{ss})^{1/2}; \sigma_{sp} = (\sigma_{pp}\sigma_{ss})^2 \quad (4)$$

where the subscripts “p” and “s” refer to protein or solvent, respectively.

The macromolecule can be solvated by a large box (cubic, rectangular, or truncated octahedron) filled of solvent molecules; the whole system can be replicated in three dimensions and treated with periodic boundary conditions.⁸⁴ Other approaches which treat only a region of the protein including the solvent in an explicit way, the remaining being represented as a reservoir and treated in the framework of stochastic boundary conditions were developed.⁹⁴

To start a dynamics simulation, an initial set of atomic coordinates and velocities are required. The coordinates can be obtained from X-ray crystallographic or NMR structure data or by model building approaches. Given a set of coordinates, the structure is first refined to relieve local stresses. Next, atoms are assigned velocities taken random from a Maxwellian distribution at a fixed temperature. Then a simulation is performed by determining the acceleration \mathbf{a}_i of atom i from Newton’s law: $\mathbf{a}_i = \mathbf{F}_i/m_i = -\nabla\mathbf{r}_i/U/m_i$. If the position of $\mathbf{r}_i(t)$ is known, the velocities $\mathbf{v}_i(t)$ and the accelerations $\mathbf{a}_i(t)$ of each atom in the system at a time t and the position of atom i after a time step Δt is given by

$$\mathbf{r}_i(t + \Delta t) = \mathbf{r}_i(t) + \mathbf{v}_i\Delta t + 1/2\mathbf{a}_i(\Delta t)^2 + \dots \quad (5)$$

Different methods for numerically approximating eq 5 were developed: e.g., the Verlet method,⁹⁵ the Beeman method,⁹⁶ the Gear method.⁹⁷ The most used is that of Verlet; with the equations for advancing the position being based on the positions from the two previous steps and from the acceleration at the previous step:

$$\mathbf{r}_i(t + \Delta t) = 2\mathbf{r}_i(t) - \mathbf{r}_i(t - \Delta t) + \mathbf{a}_i(\Delta t)^2 + \dots \quad (6)$$

Such an algorithm can be easily modified to introduce constraints on internal coordinates, such as bond lengths and angles. Actually, in protein systems, to reduce computer time and to preserve an appropriate structure, the bonds can be constrained to a fixed length by the SHAKE algorithm, an iterative procedure that adjusts, after each step, the atomic positions in succession, to simultaneously satisfy all the constraints within a specified tolerance.⁹⁸

MD simulation approaches were first performed by keeping the energy constant (microcanonical or NVE ensemble). Successively, to better match the experimental conditions, methods to simulate at constant temperature (canonical or NVT ensemble) or both pressure and temperature constant (isobaric–isothermal or NPT ensemble) were developed. Indeed, the study of temperature and pressure dependent properties of biological systems has been growing in importance. Andersen originally proposed a method for a constant pressure.⁹⁹ In his approach, the volume of the system was a dynamical variable while the generalized force acting on this variable was proportional to

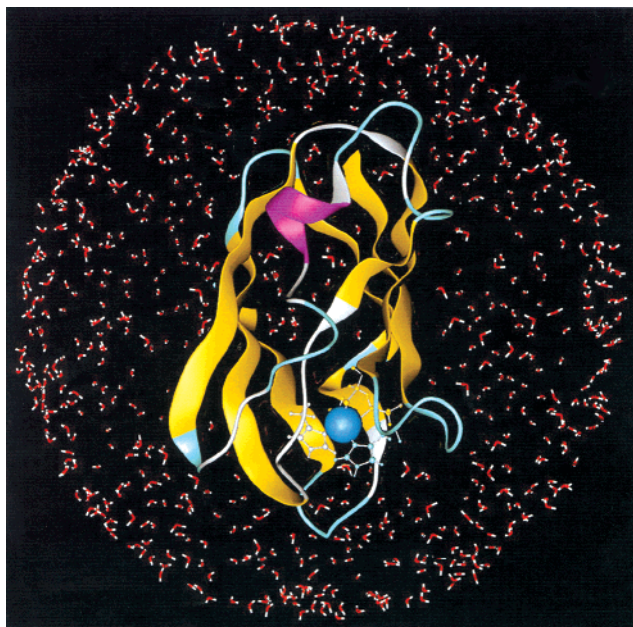


Figure 1. X-ray structure of plastocyanin, a copper containing protein involved into the photosynthetic process, with the 3514 water molecules. The drawing, generated with crystallographic coordinates from ref 201 and using the program Quanta, describes the system in the starting conditions before performing a MD simulation.

the difference between the internal and external fixed pressure. The fundamental idea of his method was to represent the effect of a suitable external reservoir by adding new degrees of freedom to the system and solving the corresponding equations of motion. One of the most popular approaches applied to protein MD simulations is that of Berendsen et al., which is based on a modified Langevin equation of motion in which the stochastic force is eliminated and the constant friction term is replaced with a variable friction proportional to the constraint.¹⁰⁰ Another approach for conducting simulation at equilibrium constant pressure was developed by Hoover.^{84,101}

Finally, it should be remarked that a particular care is to be devoted to the equilibration procedure. Indeed, before collecting data for analysis, a MD simulation run, until monitored quantities have been properly equilibrated, is to be performed.⁸⁴

3. Structural and Dynamical Properties of Hydration Water at the Protein Surface

3.1. General Considerations. Water molecules at the protein–solvent interface form irregular networks, persisting even beyond the first solvation shell, whose details depend on the subtle aspects of the protein structure and amino acid composition.^{1,2,102} From a general point of view, the effects induced by the protein macromolecule on the surrounding water can be considered in two ways.²⁰ As a protein displays on its surface a variety of functional groups with different physicochemical properties, hydration water can be studied on a full-detail accounting for local differences in the mutual influence of solute and solvent. Alternatively, the protein can be considered as a whole, and the solvent distribution can be monitored in a spatially averaged manner, i.e., as a function of the distance from the protein surface.

3.2. Solvent Accessible Surface. With the exception of water molecules occupying internal cavities, hydration water surrounds the protein surface by interacting with the biomolecule atoms exposed to the solvent (see Figure 1). There are essentially two types of protein side chains: hydrophilic side chains that are

relatively soluble in water and hydrophobic side chains that are less soluble and tend to cluster together in the protein interior.¹⁰³ The balance between the various forces involved into the protein–protein and the protein–solvent interactions is crucial to determine the secondary and the tertiary structure of proteins as well as the folding path. An useful indicator of how a surrounding medium affects protein structures is represented by the surface area of protein atoms in contact with the solvent molecules: the so-called solvent accessible surface (SAS).^{104,105} Such a quantity, describing the extent of the exposure of protein atoms to solvent, is particularly relevant for the study of the protein folding, of the crystal packing, of the molecular recognition, and of the protein–protein interactions.¹⁰⁶

A variety of computational methods were developed to evaluate the area over which contact between protein and solvent can occur.^{104–107} Generally, SAS can be defined as the area traced out by the center of a probe sphere (representing a solvent molecule) as it is rolled over the van der Waals surface of the biomolecule.^{104,107} SAS can be alternatively evaluated by adding the radius of a solvent molecule to the atomic radii and then calculating a dot surface representation.¹⁰⁸ A different approach to evaluate the real solvent-covered surface area of a protein can be obtained by monitoring the number of water molecules that are found at each protein atom for a given time interval.¹⁰⁹

The analysis on a number of proteins revealed that the SAS of a protein in an aqueous medium mainly depends on the number of protein atoms.¹⁰⁶ Conversely, a comparison of the SAS of a protein embedded in an aqueous medium or in an organic solvent showed differences depending on the residue character:¹¹⁰ a large increase in SAS was observed for polar and charged side chains upon moving from chloroform to water.

It is worth noting that the SAS of many different globular proteins, showing some kind of roughness, or self-similarity, was modeled as a fractal surface with a dimension larger than 2.^{111,112} Such a property of the protein surface has been suggested to be of some relevance for the biological functionality: a fractal surface dimension larger than 2, can affect the diffusive properties of the surrounding solvent (see section 3.7); therefore, an acceleration of the capture of the substrate from the bulk, with a concomitant slowing down of the migration of the substrate along the protein surface could occur.^{111,113}

3.3. Radial Distributions and Hydration Sites. The structural organization of water at the protein interface can be described by the so-called protein–solvent radial distribution function representing the relative probability of finding any solvent molecule whose oxygen is at a distance r from a specific solute atom.^{16,18,114–117} At a basic level, the distribution function $g_{\alpha}(r)$ can be expressed by¹¹⁷

$$g_{\alpha}(r) = \frac{\langle \Delta N(r) \rangle}{4\pi r N_W \rho \Delta r} \quad (7)$$

where r is the distance between the protein atom α and the solvent oxygen, $\langle \Delta N(r) \rangle$ is the number of solvent molecules in the region between $r - \Delta r/2$ and $r + \Delta r/2$ averaged in time, N_W is the total number of water molecules present in the system, and ρ is the density of bulk water.

More accurately, the protein–solvent radial function $g_{\alpha}(r)$ is given by¹¹⁸

$$g_{\alpha}(r) = \frac{\sum_{i=0}^{t_{\text{run}}} \sum_{j=1}^{N_W} \delta(|\mathbf{r}_{\alpha} - \mathbf{r}_j| - r)}{N_W d\tau_{\Omega}(r,t)} \quad (8)$$

where t_{run} is the simulation length, $\delta(r)$ is the delta function

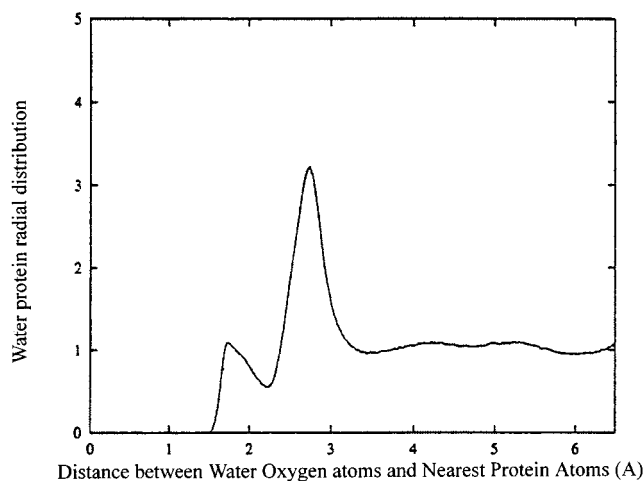


Figure 2. Water–protein radial distribution around equilibrated myoglobin as a function of the distance between water oxygen atoms and the nearest protein atoms, including hydrogen atoms. Adapted from ref 119.

centered at the site r , and \mathbf{r}_α and \mathbf{r}_j are the protein atom and the oxygen water locations, respectively; $d\tau_\Omega(r,t)$ is the normalization volume that accounts for the presence of the other protein atoms and whose time dependence arises from the protein conformational fluctuations.

The solvent distribution function around a protein atom, perpendicular to the protein surface, $g_\perp(r)$, can be derived from eq 8 by determining for each solvent molecule j , the distance $|\mathbf{r}_\alpha - \mathbf{r}_j|$ from the closest protein atom α .^{20,118}

The radial distribution function of water around a protein macromolecule generally reveals two peaks^{16,46,115–119} (see, as an example, Figure 2). The first one, at about 1.5–2 Å, arises from the strong interaction between the water oxygen atoms with the hydrogen bond acceptor groups on the protein surface.^{16,119} The second peak, whose location ranges between 2.5–3.5 Å according to the protein system, is due to the interaction between water molecules and the nonhydrogen atoms of the protein,^{16,117–119} the position of such a peak being also dependent on the particular protein atom type. The bulk limit for the radial distribution is generally reached for distances greater than 10 Å from the protein surface; such a result supporting the persistence of water structural organization beyond the first layer of hydration.¹¹⁸

The clustering of water molecules close to the protein surface, resulting in a local increase of water density, led to the introduction of the concept of the hydration site. Accordingly, a hydration site can be defined as being a local maximum in the solvent density close to the protein surface.^{120,121} The calculation of the water density may follow two different criteria.²⁰ The first one introduces a radial pair distribution function of water oxygen atoms around the atom types on the protein surface and the extent of the solvation shell is determined by considering a suitable cutoff radius^{16,17,118,122,123} Such an approach introduces a set of atom type-specific parameters, but instantaneous fluctuations in the water molecule configuration around a surface protein atom are not taken into account. Therefore, hydration sites result to be as local maxima in the time-averaged solvent density.^{120–122,124} Alternatively, the instantaneous positions of the solvent molecules are used for the determination of the solvation shell. This holds for the Voronoi polyhedra method, a geometrical procedure that does not make use of any parameter, and consists of the evaluation of a distribution function for oxygen water around a protein site.¹²⁰

Furthermore, the hydration site, sometimes called the first coordination shell, of a protein atom can be defined as a sphere of radius $\mathbf{r}_{\text{shell}}$ given by¹²⁵

$$\mathbf{r}_{\text{shell}} = \mathbf{r}_{\text{min}} + \mathbf{r}_{\text{OH}} + \Delta\mathbf{r}_{\text{RT}} \quad (9)$$

where \mathbf{r}_{min} is the minimum exclusion distance between the solute and the water oxygen atoms, \mathbf{r}_{OH} is the O–H bond length in a water molecule, and $\Delta\mathbf{r}_{\text{RT}}$ is a correction term to take into account for positional thermal fluctuations.

In general, the collection of hydration sites does not appear as an uniform monolayer at the protein surface but as a patchwork of water clusters.^{119,122} Regions with tightly clustered water molecules together with low-density areas can be observed.^{16,46,119,122} It should be noted that low density areas cannot be associated to a particular residue class since charged and polar together with hydrophobic residues are commonly found within these regions.¹²²

A comparison between MD simulation results and experimental data reveals an uncomplete matching between hydration sites and crystallographic waters.^{119,120,122} A probable reason for such a discrepancy may reside in the absence of crystal packing effects in the simulation¹²² or in the absence of solvent fluctuations in connection with protein motions.¹²⁰

3.4. Hydrogen Bond Analysis. Hints on the structural and dynamical organization of water at the protein–solvent interface can be obtained by analyzing the protein–solvent H-bond network.^{16,110,119,126–129} The presence of hydration water, which partially competes with protein atoms in the formation of H-bonds, globally affects the intramolecular H-bonds. Geometric or energetic criteria were adopted to define the formation of a H-bond during the MD simulation. A geometric criterion is satisfied if the hydrogen to acceptor distance is shorter than a fixed value (e.g., 0.32 nm) and the donor–acceptor angle was larger than a given value (e.g., 120°).^{126,127} Alternatively, it can be assumed that two water molecules are hydrogen bonded if their interaction energy is lower than a threshold (e.g., –10 kJ/mol).^{130–132}

Analysis of the H-bond network commonly involves the determination of the average number of H-bonds $\langle N_{\text{hb}} \rangle$ formed between the protein and the surrounding water molecules:¹²⁶

$$\langle N_{\text{hb}} \rangle = \frac{N_{\text{hb}}}{N_{\text{step}}} \quad (10)$$

where N_{hb} is the total number of H-bonds that are found during the analyzed period and N_{step} is the number of trajectory frames. The H-bond average lifetime τ_{H} can be calculated by the following expression:¹²⁶

$$\tau_{\text{H}} = \frac{\langle N_{\text{hb}} \rangle}{N_{\text{DW}}} t_{\text{run}} \quad (11)$$

where t_{run} is the simulation length and N_{DW} is the number of different water molecules engaged in H-bonds with each amino acids residue during the time t_{run} . Alternative analysis of the H-bond network dynamics could be done by considering the correlation function of a H-bond operator $h(t)$ which takes the value of 1 when a tagged pair of atoms are bonded, 0 otherwise;¹³³ hence, the H-bond lifetime can be extracted from the relaxation of the correlation function of $h(t)$.

At sufficient hydration, an extensive hydrogen-bonded network is formed between solvent molecules and specific sites of the protein structure.^{23,128,134} In particular, water molecules

form hydrogen bonds with carbonyl and N–H groups of the backbone and with several polypeptide side chains. The breaking and forming of these hydrogen bonds was suggested to be a prerequisite for the occurrence of stochastic large amplitude motions of the macromolecule.¹³⁵

MD simulations showed that, at the protein surface, H-bonds are preferentially formed by hydrogen atoms from water as donors^{128,129} in agreement with results as obtained by NMR;²³ such an aspect seems to be connected to the high directional structure of the H-bond.¹³⁶ The average number of H-bonds ($\langle N_{\text{hb}} \rangle$) between the protein amino acids and the solvent was found to be strongly dependent on the polar character of the exposed protein atoms:¹²⁹ such a value being in a satisfactory agreement with the experimental hydration number.²³ In addition, the H-bond lifetimes τ_{H} between the protein and the solvent reveal a wide variability from 0.5 ps up to 50 ps or even more.¹²⁸ For longer times, some water molecules were considered as being practically “bound” to the protein macromolecule.

An analysis of the number of different water molecules engaged in H-bonds N_{DW} in connection with the lifetime τ_{H} , provides information about the dynamics of H-bond network at the protein–solvent interface. Large values for N_{DW} point out that a frequent exchange of water molecules engaged in the H-bonds occurs during the analyzed period.¹²⁸ On the other hand, high values for N_{DW} in connection with low values for $\langle N_{\text{hb}} \rangle$ reflect a decreased capability to form a H-bond. It is interesting to note that, while the average number of H-bonds ($\langle N_{\text{hb}} \rangle$) is only slightly affected by the hydration level, a strong decrease of the H-bond lifetime τ_{H} was detected by lowering the hydration level.¹²⁸ The finding that the H-bond network dynamics is significantly slowed at low hydration agrees quite well with the experimental evidence pointing out that a minimum amount of water is required to activate the protein functionality.

While at low temperature H-bonds are preferentially formed between the protein and the surrounding solvent, at high temperatures the formation of the intramolecular H-bonds becomes favored,⁵⁰ such a behavior being indicative that the competition between the protein and the solvent in the H-bond network formation is thermally controlled.⁵⁰ Additionally, it was found that the trend with temperature of the number of different water molecules N_{DW} engaged in the protein–water H-bonds exhibits a transition at 200–220 K (see Figure 3). It should be remarked that a similar trend was observed in the number of water molecules involved into H-bonds for SPC/E bulk water.¹³⁷ It appears quite interesting that the onset of the dynamical transitions in proteins mimics, in some way, that of water probed through the H-bond dynamics. This led some authors to suggest a coupling between the protein and the solvent dynamics.^{35,50,138} In particular, it was hypothesized that hydration water dynamics could be coupled to the motion of the polar lateral chains through an injection of fast excitations which can trigger more extensive collective motions.³⁵ These findings received an experimental support by neutron scattering data on myoglobin^{135,139} which have revealed that a discontinuity in length of the protein–solvent H-bond as a function of temperature might occur at the origin of the onset of the anharmonic protein motions at high temperature. Notably, recent MD simulation results, making use of different thermal baths for the protein and the surrounding solvent, suggested that the enhancement in the protein fluctuations magnitude above the glass-transition temperature is mainly due to the solvent mobility.⁵¹

3.5. Residence Times. Water residence times could provide useful insights into the structural and dynamical behavior of

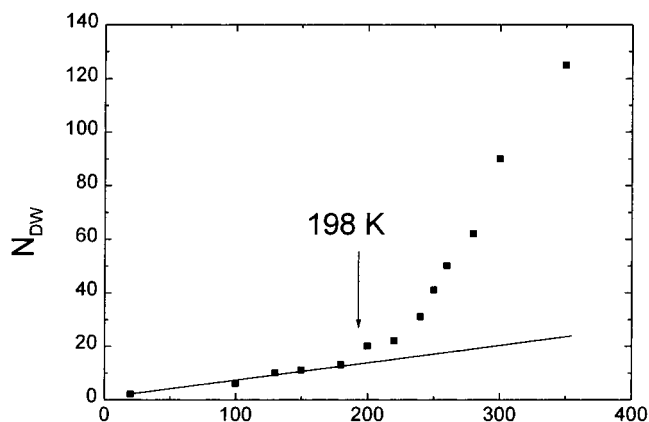


Figure 3. The number of different water molecules N_{DW} engaged in protein–water H-bonds as a function of temperature. The solid line represents the harmonic trend obtained by a linear fit from 20 to 180 K. The temperature at which the dynamical transition occurs is also shown. Adapted from ref 50. The data have been obtained from a MD simulation by GROMOS, in a canonical ensemble, of plastocyanin with 230 water molecules; a cutoff radius of 1.4 nm for the electrostatic interactions has been used. The system has been equilibrated for 100 ps followed by 500 ps of data collection.

interfacial water in the first, or successive, hydration shells of protein atoms exposed to the solvent.^{17,18,124,127,140,141} This approach results to be particularly useful to investigate the dynamical behavior of those water molecules so closely associated with the protein that their behavior sometimes can no longer be described simply as diffusive. The mean residence time $\tau_{\text{mean}}(\alpha)$ may be determined at each hydration site by averaging the time periods τ_j during which a single distinct water molecule j was residing within a small given distance from the protein site α :¹⁰⁹

$$\tau_{\text{mean}}(\alpha) = \frac{1}{N_{\text{W}}} \sum_{j=1}^{N_{\text{W}}} \tau_j(\alpha) \quad (12)$$

where N_{W} is the total number of water molecule, with the sum including only water molecules within a fixed distance from the protein atom α .

More commonly, the residence time was evaluated from a survival time correlation function $C(t)$,^{17,125,127} describing the relaxation of the hydration shells of a protein atom (or even of a layer) around the macromolecular body.¹⁴² At a protein atom α , $C_{\alpha}(t)$ is defined in terms of a binary function $p_{\alpha,j}(t, t + t'; t_0)$ that takes the value of 1 if the j_{th} water molecule stays in the coordination shell of atom α from time t to a time $t + t'$ without getting out, in the interim, of this interval, (except for a short interval of time t_0) and takes the value of zero otherwise. Formally,^{140,143}

$$C_{\alpha}(t) = \sum_{j=1}^{N_{\text{W}}} \frac{1}{t_{\text{run}} - t} \sum_{t'=0}^{t_{\text{run}} - t} p_{\alpha,j}(t, t + t'; t_0) \quad (13)$$

where N_{W} is the total number of water molecules in the system and t_{run} is the length of the simulation time t_0 ; $C_{\alpha}(t)$ gives the average number of water molecules that still remain in the coordination shell of the site α after a time t . In addition, the survival time correlation function can be also defined by taking into account, instead of the site α , a layer of thickness R around the protein body defined as the volume including all water oxygens whose minimum distance to any protein atom is less than or equal to R ;¹⁴⁰ such a quantity can be indicated by C_{R}

(t). The value assumed for $t = 0$ is a measure of the coordination number of the site and represents the average number of water molecules residing in the hydration shell of α , or in the layer R .¹²⁷

The relaxation trend of the $C_{\alpha}(t)$ provides information about the local dynamics of hydration water. In analogy with what was done in the case of water molecules solvating simple ions,^{125,127} the survival time correlation functions can be approximated by a single-exponential function:

$$C_{\alpha}(t) = Ae^{-t/\tau_{\alpha}} \quad (14)$$

Fitting data with eq 14 provides the relaxation time τ_{α} which represents the water mean residence time at the protein atom α . In many cases, a better fit of the survival time correlation function was obtained by using a double exponential,^{122,142}

$$C_{\alpha}(t) = Ae^{-t/\tau_{\text{as}}} + Be^{-t/\tau_{\text{al}}} \quad (15)$$

where τ_{as} and τ_{al} are a short and a long time decay constant, respectively. These decays correspond to solvent molecules that stay in the hydration shell for prolonged periods of time or enter and then immediately leave out. Other approaches to describe the survival time correlation functions used a multiexponential function.^{127,140}

The residence times of water at the protein–solvent interface, as calculated by the different approaches outlined above, exhibit a high variability in their values, irrespectively of the specific analyzed protein.^{17,20,109,120,122,127,140} Usually, time residence values ranging from 0.5 to 50 ps are observed for various protein sites.^{20,127,140} Moreover, a significant number of water molecules with a residence time in the 100–500 ps time scale was also found.¹²⁷ Analysis of these residence times, as a function of the amino acid residue types, suggests a dependence on the polar or charged character of the protein residue. In particular, the following ranking relationship for τ_{α} was observed for crambin,¹²⁷ plastocyanin,¹⁴⁰ and azurin¹⁴⁴ according to the chemical character of the residue: $\tau_{\text{charged}} \geq \tau_{\text{polar}} > \tau_{\text{non polar}} \approx \tau_{\text{bulk}}$ (τ_{bulk} being the residence time of bulk water). However, for bovine pancreatic trypsin inhibitor, such a relationship among polar, charged and non polar residues was not obeyed.^{17,109} Finally, even if the residence times should be, in some way, controlled by the H-bond network dynamics, a simple correlation between τ_{α} and H-bond average lifetime τ_{H} cannot be found.^{109,140} It should be remarked that the residence times around proteins, assuming a wide range of values, follow a power law distribution.^{142,143} Such a trend was indicative of the fact that a sort of temporal disorder characterizes the protein–solvent interface.¹⁴⁵

Furthermore, water molecules solvating a protein have drastically different coordination numbers. Actually, while water molecules in the protein interior have a coordination number from zero to three, external water molecules are characterized by a number from zero to twelve.¹⁴³

The relaxation trend of the survival time correlation functions, depending on the mechanisms regulating the protein–solvent interactions, can provide additional information about the dynamical character of interfacial water.^{17,127,140} The time decays of the survival time correlation function $C_{\text{R}}(t)$ of water belonging to layers with a radius R far from the protein surface are well-approximated by a single exponential relaxation. On the contrary, a nonexponential time behavior was recorded as far as water layers progressively closer to the protein surface are taken into account. In particular, the relaxation $C_{\text{R}}(t)$ of water in the proximity of the protein surface can be accurately described by a stretched exponential or a Kohlraush–Williams–

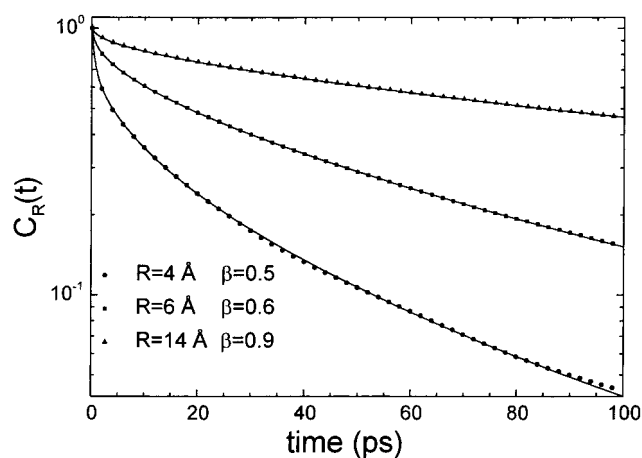


Figure 4. Semi-log plot of the survival time correlation function $C_{\text{R}}(t)$ of hydration water around a hydrated protein by restricting the analysis to water molecules moving within regions characterized by different distances R from the protein surface: dots ($R = 4 \text{ \AA}$), squares ($R = 6 \text{ \AA}$), and up triangles ($R = 14 \text{ \AA}$). The solid lines are the fitting curves obtained by eq 16. Adapted from ref 142. The data have been obtained from a MD simulation by GROMOS, in a canonical ensemble, of plastocyanin with 3514 water molecules with periodic boundary conditions; a cutoff radius of 1.4 nm for the electrostatic interactions has been used. The system has been equilibrated for 100 ps followed by 1000 ps of data collection.

Watts function (KWW):^{20,122,127,142,146}

$$C_{\text{R}}(t) = Ae^{-(t/\tau_{\text{R}})^{\beta}} \quad (16)$$

where τ_{R} provides the time scale over which the process evolves and gives an estimate of the residence time of waters in the considered solvent layer; the stretching parameter β is a signature of the nonexponential trend of the phenomenon. The deviation from a single-exponential time behavior increases in the vicinity of the protein surface (see Figure 4): β values shifting from the bulk value (about one) up to 0.5 in the first hydration shell.^{20,127,142} If we consider that the stretched exponential functions are commonly used to describe the relaxation in amorphous, disordered systems,^{147,148} the above-reported behavior for the survival distribution function may constitute an additional phenomenological indication of the glassy character of hydration water. On the other hand, the appearance of stretched exponentials can be connected to the spread in the residence time values.¹⁴⁹ Indeed, a residence time distribution, which reflects a heterogeneity in the temporal behavior of hydration water, might be put into a relationship with the peculiar relaxation dynamical behavior through a spread in the barriers of the energy landscape.^{150,151}

All these features suggest that the water dynamical behavior close to the protein surface appears to be reminiscent of that observed in protein systems.^{29,152,153}

3.6. Diffusion Coefficient. Water mobility in the proximity of the protein surface exhibits a wide range of dynamical behaviors: from very tightly bound water to extremely mobile water diffusing on the protein surface. A good reporter of this mobility is represented by the self-diffusion coefficient which is widely used in both spectroscopic investigations^{154,155} and MD simulation approaches⁸⁴ of liquids.

The self-diffusion coefficient D (or, commonly, the diffusion coefficient) can be calculated by integration of the unnormalized velocity autocorrelation $C_{\text{vv}}(t)$:

$$D = \lim_{T_c \rightarrow \infty} \frac{1}{d} \int_0^{T_c} C_{\text{vv}}(t) dt \quad (17)$$

where d is the spatial dimension and $C_{vv}(t)$ can be calculated by

$$C_{vv}(t) = \frac{1}{N_W} \sum_{i=1}^{N_W} \frac{1}{t_{\text{run}} - t} \int_0^{t_c} \mathbf{v}_i(t + \tau) \mathbf{v}_i(\tau) d\tau \quad (18)$$

where $\mathbf{v}_i(t)$ is the velocity of the i th water molecule at the time t ; N_W is the number of water molecules, and t_{run} is the total time interval.

Alternatively, the solvent mobility is conveniently described by the diffusion coefficient D related to the slope of the molecule MSD by the Einstein relationship, which, in d dimensions, is⁸⁴

$$D = \frac{1}{2d} \lim_{\Delta t \rightarrow \infty} \frac{\langle |\mathbf{r}_i(t) - \mathbf{r}_i(0)|^2 \rangle}{\Delta t} = \frac{1}{2d} \lim_{\Delta t \rightarrow \infty} \frac{\langle \Delta r^2 \rangle}{\Delta t} \quad (19)$$

where $\mathbf{r}_i(t)$ and $\mathbf{r}_i(0)$ are the position vectors of the solvent molecule i at the time t , and at the time $t = 0$, respectively; the brackets “ $\langle \rangle$ ” indicate the average over both the time origin $t = 0$ and the solvent molecules. The time interval Δt has to be large compared to the correlation time τ of the velocity autocorrelation function, so that any dynamical coherence in the motion of the molecule has disappeared.^{156,157} Actually, at very short times (less than approximately 0.2 ps), before the diffusive regime is established, the MSDs follow a ballistic regime ($\Delta r^2 \propto t^2$), followed by a transient period after which the MSD curves seem to exhibit a linear trend as a function of time.^{19,114}

Even if the values of D obtained from the autocorrelation function and those calculated from the Einstein relation do not differ by more than the error involved in the calculation of D , the latter method is less commonly used to extract the D values in water–protein systems since it requires to store data with a higher frequency.¹⁵⁸

At a large distance from the protein surface, the bulk value is generally reproduced for the diffusion coefficient; such a value depending on the used water potential model. Conversely, conflicting results are reported for D values close to the protein surface.^{16,94,109,110,114,116,118,129} Different possible causes might be invoked to explain such discrepancies. The peculiar interactions of solvent molecules with protein atoms, at the solvent interface, may introduce some irregularities in the trapping time of the water molecules. Accordingly, it can be necessary to treat the diffusion as a local property. In some cases, it was chosen to calculate the MSDs by restricting the analysis to those water molecules whose trajectories are confined within a region put at a limited fixed distance from the protein surface. On such a basis, the MSDs, and then the average values of the diffusion coefficient, are determined in radial shells or flat slabs around the protein.^{19,20,159} Alternatively, radial profiles of quantities describing water mobility as a function of the distance from the protein surface were evaluated.^{109,110,114,116,118,129,160} In this respect, different criteria to assign water molecules to a given region were applied. In particular, water molecules were assigned to a specific hydration layer depending upon their initial positions irrespectively of their successive behavior^{118,161} or, alternatively, only waters that stayed in the same layer during the period required for the analysis were considered.^{19,114}

The radial profiles of D as a function of the distance from the protein surface, as well as the values of D in radial shells around the macromolecule, reveal that solvent mobility is restricted^{19,110,114,116,118,129} or retarded.^{20,109} In particular, a decline of the diffusion coefficient values from the bulk values is generally observed as far as the protein surface is ap-

proached.^{20,94,109,114,116,117,129,162} In addition, sometimes an evidence of hypermobile water at an intermediate distance (4–8 Å) from the protein surface was detected;^{2,94,110,114,116,118,129} such a feature having been hypothesized to arise from simulation artifacts caused by truncation of the electrostatic interactions.¹⁵⁹

Furthermore, an analysis of the local mobility of the solvent in the various volume elements ΔV around specific sites at the protein surface was conducted.^{94,115,118} A local diffusion coefficient D_{uvw} at each point \mathbf{r}_{uvw} of a rectangular grid around the protein sites, whose cells are characterized by the uvw index, can be calculated according to¹¹⁸

$$D_{uvw} = \frac{1}{6(t_2 - t_1)} (\langle |\mathbf{r}(t_2) - \mathbf{r}(0)|^2 - |\mathbf{r}(t_1) - \mathbf{r}(0)|^2 \rangle) \quad (20)$$

where the point $\mathbf{r}(t)$ represents the center of a grid cell surrounding the protein and $t_2 - t_1$ is the time interval during which the water mobility is evaluated; water molecules were assigned to their particular regions depending upon their initial positions. It was found that, while the translational motion of bulk water assumes diffusive characteristics within a picosecond, a water molecule travelling along the protein surface will encounter locally changing environments that impose different rates upon its motion.¹¹⁸ Such a finding can be connected with the presence of a distribution of the hydration water residence times in the vicinity of the protein surface (see section 3.5).

Moreover, although there were done many attempts to investigate the influence of different solute chemical groups on the mobility of the surrounding solvent and, in particular, how water diffusion is affected by polar, apolar, charged protein groups, no definite conclusions were reached^{2,16,94,115,117} and sometimes conflicting results were obtained.^{2,16,94} During the temporal interval required to establish the diffusive regime, water molecules may visit different protein sites with a different polar character by affecting the final diffusive values.

To better put into evidence the influence of the protein on the diffusive properties of hydration water, an analysis of the anisotropy of the solvent diffusion was done.^{114,160,161,163,164} The MSD of water molecules can be decoupled into a parallel $\langle \Delta r_{\parallel}^2 \rangle$ and a perpendicular $\langle \Delta r_{\perp}^2 \rangle$ components relative to the protein surface:

$$\langle \Delta r^2 \rangle = \langle \Delta r_{\parallel}^2 \rangle + \langle \Delta r_{\perp}^2 \rangle \quad (21)$$

where the $\langle \Delta r_{\perp}^2 \rangle$'s can be calculated from the displacement, along the normal, to the protein surface of water oxygen from the closest protein atom; the $\langle \Delta r_{\parallel}^2 \rangle$'s can be derived from the total MSDs. According to eq 19, a decoupling of the diffusion coefficient into a parallel and a perpendicular component with respect to the protein surface can be done.^{114,161,163,164} The diffusion rate perpendicular to the solute surface is found to be slower in comparison to the overall diffusion, whereas diffusion parallel to the solute surface is faster; such an effect, progressively decreasing with the distance from the protein macromolecule, disappears at about 15 Å from the solute.^{114,161,163,164} The relative increase in the parallel component of D can be viewed as a consequence of the equipartition of energy principle.¹⁶¹ The anisotropy in the diffusive dynamics of water, confirmed by experimental results,^{154,155} might be connected to the structural organization of the water molecules at the protein–solvent interface resulting into a preferential orientation of the water electric dipole with respect to the normal to the protein surface (see also the section 3.8). On the other hand, we remark that fast diffusion along the protein surface could accelerate the

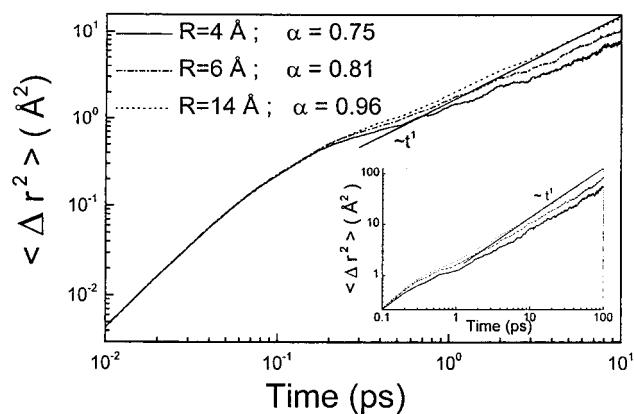


Figure 5. Mean square displacements of water molecules versus time around a fully hydrated plastocyanin by restricting the analysis to water molecules moving within regions characterized by different distances R from the protein surface: $R = 4 \text{ \AA}$ (solid line), $R = 6 \text{ \AA}$ (dot-dashed line) and $R = 14 \text{ \AA}$ (dotted line). Each curve was obtained by averaging over 20 different time origins and over the corresponding water ensemble. The values of α reported in figure were extracted by a fit of the curves, in the time interval from 1 to 10 ps, according to eq 22. The heavy line indicates a trend of $\langle \Delta r^2 \rangle$ as $\sim t^1$. Inset: mean square displacements for the same water ensemble in the time interval 0.1–100 ps. Adapted from ref 142.

migration of the substrate and then result into an enhancement of the rate of binding to the active site.^{111,163}

3.7. Anomalous Diffusion. An additional possible cause for the discrepancies observed in the water diffusion coefficient values, at the protein–solvent interface, is the occurrence of anomalous diffusion. Indeed, the use of the Einstein relationship (eq 19) for the determination of D presumes a linear increase of the diffusing particle MSD with time. This condition, which is usually fulfilled for most homogeneous isotropic three-dimensional liquids on time scales longer than a few picoseconds, does not hold for water molecules diffusing around a protein.¹⁹ Actually, a sublinear trend was detected for the MSDs of water molecules moving close to the plastocyanin surface. After the break from the ballistic regime, the $\langle \Delta r^2 \rangle$'s follow the law^{19,163}

$$\langle \Delta r^2 \rangle \approx t^\alpha \quad (22)$$

where the α exponent results to be smaller than one.¹⁹ Such a trend can be easily visualized in the log–log plot resulting into linear behavior in time (see Figure 5). In addition, as long as larger distances from the protein surface are taken into account, the α exponent is found to approach to one^{19,142} (see the α values in Figure 5). Generally, deviations of the α exponent from 1 is indicative of anomalous diffusion. Occurrence of anomalous diffusion in the proximity of the protein surface was experimentally confirmed by neutron scattering on hydration water around myoglobin.⁶⁰

In the presence of anomalous diffusion, the slope of $\langle \Delta r^2 \rangle$ changes with time, and an evaluation of D by means of eq 19 could lead both to an incorrect and t -dependent value for D . This fact might be at the origin of the numerous discrepancies found in the water diffusion coefficient evaluations, especially when an analysis of D as a function of the distance from the protein is performed.^{16,94,109,110,114,118,129} In this context, some caution was suggested in the use of the self-diffusion coefficient to characterize the water dynamics in protein systems.¹⁹ Alternatively, an effective diffusion coefficient D_{eff} , depending on the travelled distance, can be introduced:¹⁶⁵

$$D_{\text{eff}} = \frac{d\langle \Delta r^2 \rangle}{dt} \approx \langle \Delta r^2 \rangle^{(\alpha-1)/\alpha} \quad (23)$$

Such an equation can provide a more reliable way to quantify, in the temporal window of interest, the water local mobility around a protein macromolecule.

The occurrence of anomalous diffusion in protein hydration water is indicative of the peculiar protein–solvent interactions and of their influence on the water dynamics. Normal diffusion, which arises from Brownian motion, can be described by a Gaussian shape for the probability distribution, or propagator $P(r,t)$, of finding a tagged particle in r at the time t , when starting at the origin at $t = 0$, is given by

$$P(r,t) = \left(\frac{1}{4\pi Dt} \right)^{d/2} e^{-dr^2/2Dt} \quad (24)$$

where d is the dimensionality of the spatial region in which the diffusion process occurs and D is the diffusion coefficient of the particles. A Gaussian propagator results into the well-known Einstein relationship (see eq 19).¹⁶⁶ Particles diffusing on a heterogeneous surface may experience a large variety of different interactions which could result into a sort of spatial and temporal disorder; such a heterogeneity could give rise to deviations from a Gaussian propagator and, consequently, eq 19 cannot be longer valid.

As already mentioned, the SAS of many different globular proteins is reminiscent of fractal surfaces with a dimension larger than 2.^{111,112} Accordingly, solvent diffusion on a protein surfaces may be affected by the spatial disorder as due to the protein roughness. The diffusive process can be then described by a non-Gaussian propagator $P(r,t)$:^{142,166}

$$P(r,t) = t^{-d_s/2} \xi^\beta e^{-a_1 \xi^\gamma} \quad (25)$$

where d_s is the spectral dimensionality of the fractal surface related to the connectivity of the structure;¹⁶⁷ $\xi = r t^{-d_s/2d_f}$ is the scaling variable assumed to be greater than one, and d_f is the fractal dimensionality of the surface; β and γ depend on the d_f and d_s .^{54,166} In this framework, the long-time limit MSD can be expressed by

$$\langle \Delta r^2 \rangle \sim t^{d_s/d_f} \quad (26)$$

Generally, since values between 1 and 2 are obtained for the spectral dimensionality d_s of protein¹⁴⁵ and values larger than 2 for d_f , it comes out that $d_s/d_f = \alpha < 1$, and then subdiffusion takes place. In other words, the occurrence of anomalous diffusion for the protein hydration water could be traced back to the roughness, or self-similarity, of the protein surface.

It can be demonstrated that a similar result can be also explained if a temporal disorder is taken into account. In short, the different interactions at the protein–solvent interface could modulate the times that water molecules spend at the various protein hydration sites. This finds a correspondence with the observed spread of the residence times.^{17,124} Therefore, the propagator results to be non-Gaussian¹⁶⁶ and the MSD's can be expressed by^{142,166}

$$\langle \Delta r^2 \rangle \sim t^{\mu-1} \quad (27)$$

where μ is a parameter related to the time distribution;^{142,166} subdiffusion being obtained for μ values smaller than 2. A confirmation to the temporal disorder picture comes from the observation that the distribution of the water residence times around a protein macromolecule follows a power law $\psi \sim 1/t^\mu$

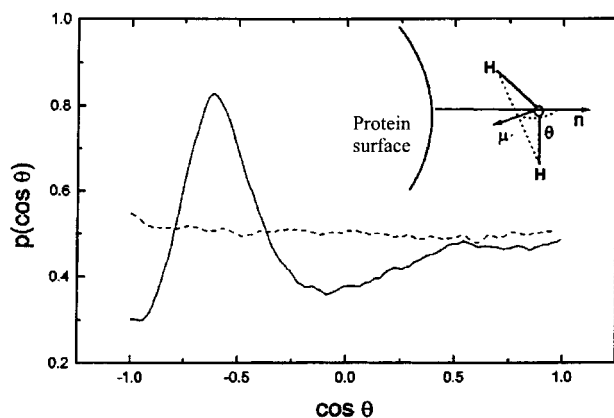


Figure 6. Distribution of cosine of the angle θ , between the normal (n) to the protein surface and the water electric dipole (μ) for water molecules whose oxygen atom is within 4 Å from the protein surface (continuous line) and within a region localized at a distance between 10 and 14 Å from the protein surface (dashed line). The water electric dipole μ is assumed to point from the oxygen atom to the center of the line joining the hydrogen atoms (see inset). Adapted from ref 142.

with a value for the μ exponent consistent with that extracted from eq 27¹⁴⁵ as expected from the related model.¹⁶⁶

Generally, the occurrence of anomalous diffusion in hydration water, arising from the peculiar interactions between the biomolecule and the solvent, can be traced back to a topological and temporal disorder closely reminiscent of an amorphous state.^{60,145} Anomalous diffusion, which constitutes a recurrent phenomenon appearing in diffusional controlled biological reactions^{19,168} could play a crucial role in regulating the biological functionality.

3.8. Water Orientation and Rotational Diffusion. The orientation of water molecules at the interface can be described by the angle θ between the electrical dipole vector μ (defined as the vector pointing from the water oxygen to the middle point between the two hydrogen atoms) and the radius vector n (from the center of mass of the protein to the oxygen in the water molecule) (see inset of Figure 6). The distribution of $\cos \theta$ of the water molecule around a protein macromolecule revealed that, while at large distances from the protein surface, all the orientations of dipoles are equally probable, close to the protein surface the electric dipole is preferentially oriented (see as an example Figure 6). In particular, it was found that in the innermost hydration layer of protein with a negative charge there was a preferential orientation of the dipole vector toward the protein surface,^{114,163} such a preference being slightly preserved in the next layer. This finding could be related to the observed anisotropy in the water diffusion around proteins.¹⁶³

Additional information about the influence of the peculiar interactions between the protein and the solvent on the diffusive properties of hydration water can arise from the study of the rotational diffusion of water. The reorientational dynamics of the water electrical dipole μ can be analyzed by means of the autocorrelation functions Γ_l defined as^{20,114,142,169}

$$\Gamma_l(t) = \langle P_l(\hat{\mu}(0) \cdot \hat{\mu}(t)) \rangle \quad (28)$$

where P_l are the Legendre polynomials of the order l and $\hat{\mu}(t)$ is the unit vector along the molecular dipole axis at time t ; the brackets “ $\langle \rangle$ ” indicate a time average. The first and the second Legendre polynomials are usually investigated; the first order can be related to the properties as derived by infrared spectroscopy, while the second one reflects quadrupolar properties that can be investigated by NMR.²⁰

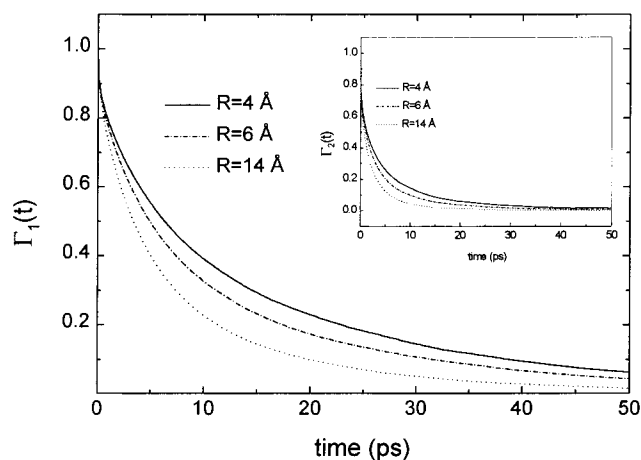


Figure 7. Rotational reorientation of the water molecule for $l = 1$, by restricting the analysis to water dipole direction molecules moving within regions characterized by different distances R from the protein surface: $R = 4$ Å (solid line), $R = 6$ Å (dot-dashed line), and $R = 14$ Å (dotted line). Inset: Rotational reorientation of the water molecule dipole direction for $l = 2$. Adapted from ref 142.

The relaxation of rotational correlation functions of protein hydration water was described by two exponential functions:^{114,116}

$$\Gamma_l(t) = Ae^{-t/\tau_{1a}} + Be^{-t/\tau_{1b}} \quad (29)$$

where τ_{1a} and τ_{1b} are the relaxation orientation times. This trend may be interpreted as arising from two processes: a fast one which accounts for the spatially restricted motion due to librational modes and another involving a rearrangement of the neighboring molecules.^{20,116} An analysis of the behavior of Γ_1 and Γ_2 showed that the reorientation diffusion appears to be retarded, with respect to bulk water, for molecules moving in the proximity of the protein surface. Such an effect was attributed to the stronger solvent–solute interactions with respect to those of water molecules farther from the macromolecule.¹⁴² In addition, the relaxation of Γ_2 occurs on a significantly faster time scale in comparison with Γ_1 (see, as an example, Figure 7).

According to what obtained for the survival time probability function, a much insightful description of the rotational relaxations was obtained by using stretched exponentials:^{20,142}

$$\Gamma_l(t) = Ae^{-(t/\tau_l)^\beta} \quad (30)$$

where β is the stretched parameter and τ_l is the orientational time. Also in this case, a deviation from a simple exponential behavior appears to be more marked in the vicinity of the protein surface, with β values ranging from 0.5 to 0.8 being observed.^{20,142} In addition, orientational times from 2 to 10 ps were detected.^{20,142}

The occurrence of stretched exponential was put into relationship, in analogy with what done for the residence time relaxations (see section 3.5), to a power law distribution of the orientational relaxation times.²⁰ This suggests that the mechanisms which govern the rotations could be strictly connected to those regulating the other dynamical processes at protein–solvent interface.

In this respect, some considerations about a possible coupling between the translational and the rotational motions were put forward. Indeed, while for normal liquids the translational and the rotational motions are practically independent, a coupling, depending on the spatial extension of the analysis, appears for

supercooled liquids.^{170,171} For protein systems, the rototranslational properties of the solvent around the protein might be strictly related to the capability of the substrate to reach and to correctly match the active site.

3.9. Dynamical Structure Factor. MD simulations can be very useful to calculate additional quantities relevant to the monitoring of the dynamical behaviors of protein systems, such as their dynamical structure factors and their intermediate scattering functions. These quantities have the additional advantage to be compared with those derived from neutron, or even Raman, scattering data. In this respect, we remark that the combination of neutron scattering and MD simulation is a powerful tool to investigate protein systems since both these approaches provide one with information covering the same spatial and temporal window.^{172,173}

Generally, neutron scattering experiments measure the total dynamics structure factor $S_{\text{tot}}(\mathbf{q}, \omega)$, where \mathbf{q} is the exchanged momentum and $\hbar\omega$ is the exchanged energy.¹⁷⁴ Such a quantity is the sum of a coherent contribution $S_{\text{coh}}(\mathbf{q}, \omega)$, arising from interference effects due to the correlations in the positions of different atoms, and an incoherent contribution $S_{\text{inc}}(\mathbf{q}, \omega)$, related to the self-correlation in the atomic positions.¹⁷⁵ The incoherent scattering of hydrogens, an order of magnitude larger than those of the other atoms, dominates the spectra profiles of protein systems.¹⁷² The incoherent dynamical structure factor $S_{\text{inc}}(\mathbf{q}, \omega)$ is proportional to the space-time Fourier transform of the self-correlation function, or Van Hove function, $g(\mathbf{r}, t)$:¹⁷²

$$S_{\text{inc}}(\mathbf{q}, \omega) = \frac{1}{2\pi} \int_{-\infty}^{+\infty} e^{(-i\omega t)} dt \int_{-\infty}^{+\infty} g(\mathbf{r}, t) e^{-i\mathbf{q}\cdot\mathbf{r}} d\mathbf{r} \quad (31)$$

where $g(\mathbf{r}, t)$ is given by

$$g(\mathbf{r}, t) = \frac{1}{N} \sum_{i=1}^N \langle \delta[\mathbf{r} + \mathbf{R}_i(0) - \mathbf{R}_i(t)] \rangle \quad (32)$$

where the sum is performed over the number N of hydrogens in the system, \mathbf{r} is a position vector, $\mathbf{R}_i(t)$ is the position vector of the i th atom at time t , and the brackets “ $\langle \rangle$ ” denote an average over time origins.

The incoherent dynamical structure factor $S_{\text{inc}}(\mathbf{q}, \nu)$ can be generally interpreted in terms of three main components, i.e., the elastic, giving information about the self-probability distributions of hydrogens, the quasielastic, related to the diffusive motions, and the inelastic one, providing information about vibrations; the relative intensity among these components depending on the temperature. From a qualitative point of view, the MD simulated $S_{\text{inc}}(\mathbf{q}, \omega)$ well reproduces the features observed in the experimental dynamical structure factor.^{63,67} By MD simulation, a particular attention was focused on the inelastic components of $S_{\text{inc}}(\mathbf{q}, \nu)$.^{63,67} Analysis of the $S_{\text{inc}}(q, \nu)$ (where q denotes the modulus of \mathbf{q}), as derived by MD simulation, of protein hydration water revealed (see Figure 8) that at temperatures up to 180 K a broad inelastic bump appears well visible in the low-frequency region, peaking at about 1.3 meV.^{62,63} By increasing the temperature, this peak becomes less and less distinct due to the raising intensity of the quasielastic contribution. The observed peak represents an excess of vibrational states over the flat Debye level. Actually, the frequency dependence of the dynamical structure factor in the inelastic region can be cast in the form $\sim 1/\nu m(\nu, T)g(\nu)$, where $n(\nu, T)$ is the Bose factor and $g(\nu)$ is the density of states. In the Debye approximation and at low frequency, $g(\nu)$ turns out to

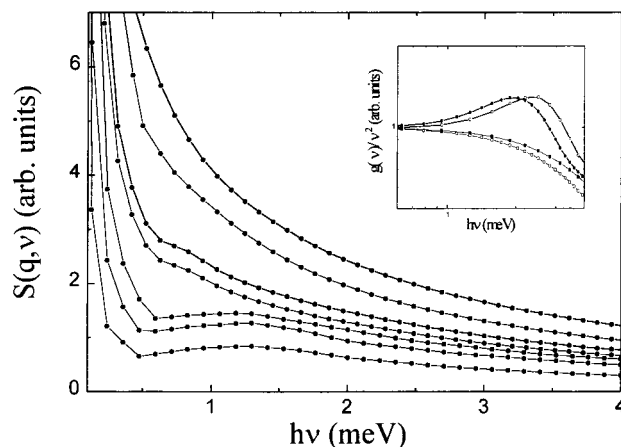


Figure 8. Incoherent dynamical structure factor $S_{\text{inc}}(q, \nu)$ of protein hydration water at a fixed q value ($q = 2 \text{ \AA}^{-1}$). The temperatures are 100, 150, 180, 200, 220K, 260, and 300 K from bottom to top. Inset: Density of states (see eq 33) divided by ν^2 , as a function of energy, at 100 K (white circles), 180 K (black circles), 200 K (black squares), and 220 K (white squares). Solid lines are a guide to eye. Adapted from ref 54.

be proportional to ν^2 and $n(\nu, T) = [e^{(\hbar\nu/k_B T)} - 1]^{-1}$ can be approximated by $k_B T/\hbar\nu$; accordingly, a constant trend as a function of frequency is expected for the dynamical structure factor. Indeed, the presence of this peak, commonly called boson peak, can be also visualized, below 200 K, in the density of states.⁶⁵ Under the assumption that the short time behavior of hydration water can be described as independent harmonic oscillators (oscillatory motion in the cage formed by its neighbors), the density of states $g(\nu)$ of hydration water can be computed as the Fourier transformation of the velocity autocorrelation function $C_{vv}(t)$ (see eq 18):

$$g(\nu) = \frac{1}{2\pi} \int_{-\infty}^{\infty} C_{vv}(t) e^{(-i\omega t)} dt \quad (33)$$

The velocity autocorrelation function $C_{vv}(t)$, which displays damped oscillations typical of liquid water, decays to zero within a short time (less than 0.5 ps).^{62,63} The density of states of protein hydration water shows a small peak assigned to translational motion at 6 meV and a more pronounced broad librational peak centered at about 50 meV.^{63,142} In addition, it reveals a bump at about 1.3 meV for temperatures below 180 K, while at higher temperatures (between 220 and 300 K), a Debye-like behavior is registered in the low-frequency region (see inset of Figure 8).

An additional interesting quantity related to the hydration water⁶⁰ is the imaginary part of the dynamical susceptibility $\chi''(q, \omega) = \nu S_i(q, \omega)$. Such a quantity provides information on diffusive motions over a broad frequency range that cannot be revealed in the $S_{\text{inc}}(q, \nu)$ representation. Generally, $\chi''(q, \omega)$ exhibits, at 100 K, four principal peaks (see Figure 9): the water vibrational one near 60 meV, a translational intermediate peak approximately at 24 meV, a broad translational peak at 4 meV, and the slow motion peak (α peak) at very low frequencies.^{62,63} A slight dependence on temperature characterizes the behavior of the dynamical susceptibility in the high energy region (> 1 meV); a small downward shift of the peaks being registered as the temperature increases. On the contrary, a strong dependence on T occurs in the lowest energy region, as it can be especially inferred from the large variability of the lowest frequency minimum. The MD calculated χ'' of protein hydration water

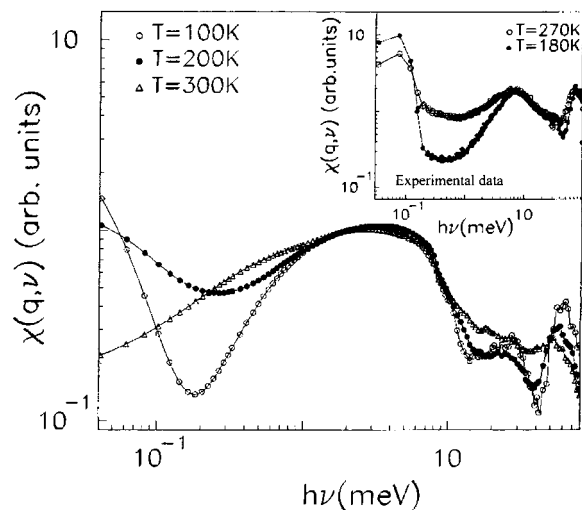


Figure 9. Calculated dynamical susceptibility $\chi''(q, \nu)$, of hydration water around plastocyanin for $q = 2 \text{ \AA}^{-1}$, at $T = 100 \text{ K}$ (white circle), 200 K (black circle), and 300 K (white triangle). Inset: experimental dynamical susceptibility of myoglobin at 270 K (white circle) and at 180 K (black circle) (data from ref 60. Adapted from ref 62.

around different proteins^{62,63} results in a good qualitative agreement with that measured by neutron scattering for water around myoglobin⁶⁰ (see inset of Figure 9). All the four peaks observed by MD simulation are also registered in the experimental χ'' of myoglobin hydration water even if at slightly different positions.⁶⁰

It is worth of note that the existence of the boson peak in the protein hydration water was first predicted by MD simulation⁶² and, subsequently, confirmed by neutron scattering measurements.⁶⁹ Notably, a similar vibrational anomaly was also detected in supercooled water confined in a pore of Vycor glass.¹⁷⁶ Furthermore, it should be remarked that the MD simulated boson peak was found at an energy (1.3 meV) lower with respect to the experimental one (about 3 meV). Such a discrepancy can be overcome if the Ewald summation to treat the long range interactions is introduced,¹⁷⁷ or alternatively, if a few proteins are inserted in a monoclinic cell filled by water molecules,¹⁷⁸ notably, both the approaches taking into account for intermolecular interactions.

Such a vibrational anomaly, whose origin is still debated, is a feature shared by many glassy systems^{38,179} and generally attributed to the topological disorder of the systems.⁶⁴ It might originate from structural correlations over an intermediate range scale, associated with localized excitations. The appearance of such an inelastic feature in protein hydration water is particularly relevant in connection with the fact that a similar vibrational anomaly was also detected in several globular proteins by both experimental investigations^{67,180,181} and MD simulation.^{63,67,182} Indeed, the simultaneous presence of a boson peak in the protein and in the hydration water, occurring at similar energies was suggested to reflect an extensive dynamical coupling between the protein and the hydration solvent. The intimate dynamical exchange between the solvent-exposed protein residues and the water molecules could be at the origin of the peculiar spectral features of both the systems. Such a picture finds a correspondence with the possibility, already mentioned, that the solvent water could “inject” its dynamics into the protein side chains.³⁵

3.10. Intermediate Scattering Function. In the temporal domain, additional information about the water dynamical behavior can be inferred by the incoherent intermediate scat-

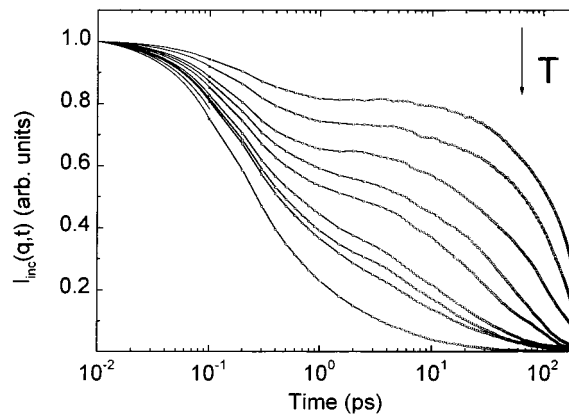


Figure 10. Intermediate scattering function $I_s(q, t)$, as a function of time, of water oxygens around plastocyanin, at a fixed q value ($q = 2 \text{ \AA}^{-1}$) for different temperatures: 100, 150, 180, 200, 220, 240, 250, 280, and 300 K from top to bottom. All the curves have been normalized to 1 at $t = 0$. Adapted from ref 54.

tering function, $I_{\text{inc}}(\mathbf{q}, t)$ given by the spatial Fourier transform of the self-correlation function $g(\mathbf{r}, t)$:^{62,172,173,182}

$$I_{\text{inc}}(\mathbf{q}, t) = \frac{1}{2\pi} \int_{-\infty}^{+\infty} g(\mathbf{r}, t) e^{-i\mathbf{q}\cdot\mathbf{r}} d\mathbf{r} \quad (34)$$

which, by eq 32, leads to

$$I_{\text{inc}}(\mathbf{q}, t) = \frac{1}{N} \sum_{i=1}^N \langle e^{i\mathbf{q}\cdot\mathbf{R}_i(t)} e^{-i\mathbf{q}\cdot\mathbf{R}_i(0)} \rangle \quad (35)$$

where the brackets “ $\langle \rangle$ ” denote an average over time origins. $I_{\text{inc}}(q, t)$ can be directly calculated from the MD trajectories of the water oxygen atoms through the relationship

$$I_{\text{inc}}(q, t) = \frac{1}{3N} \sum_{i=1}^N \langle e^{i\mathbf{q}\cdot[\mathbf{R}_i(t) - \mathbf{R}_i(0)]} \rangle \quad (36)$$

where N is the total number of water atoms in the sample and the brackets “ $\langle \rangle$ ” denote an average over both the time origin and the exchanged momenta \mathbf{q} having the same modulus q to take into account anisotropic effects. Usually, the slowly decaying tail of $I_{\text{inc}}(q, \nu)$ is multiplied by a Gaussian damping envelope to overcome spurious effects due to truncation.¹⁷³

First we note that at low temperatures, slight oscillations, well-distinct from the noise background, can be observed in the $I_{\text{inc}}(q, t)$ curves (see as an example Figure 10). Such an effect was recently interpreted as a time domain manifestation of the boson peak,¹⁸³ even if a great caution was suggested in attributing a physical relevance to such a kind of oscillations; they could originate from some simulations artifacts such as a finite size effect arising from a disturbance that propagates through the system leaving and reentering the boundaries of the periodic box at the sound velocity.¹⁸⁴

The temperature dependence of the $I_{\text{inc}}(q, t)$ related to the hydration water close to the protein surface reveals a two-step decay (see as an example Figure 10).^{54,63} The fast relaxation is distinctly separated from the slow one by a plateau,⁵⁴ such a distinction becoming progressively less evident as the temperature increases. It is interesting to observe that the time scale of the initial decay was found to strongly depend on the water model: for the TIP3P model it is 10 times faster with respect to the SPC/E.⁶³

The two-step decay can be put into relationship to a dephasing of librational-translational modes and slow diffusive displace-

ments,^{60,63} in agreement with what suggested for supercooled bulk water.¹⁷⁰ In addition, the long time decay of the hydration water $I_{\text{inc}}(q,t)$ appears to be nonexponential,^{54,63} in agreement with what observed in the experimental data,⁶⁰ and matches a KWW function:

$$I_{\text{inc}}(q,t) = Ae^{-(t/\tau_{\text{relax}})^\beta} \quad (37)$$

where τ_{relax} is the relaxation time and β is the stretched parameter, with the deviation of β from 1 becoming more marked as the temperature is increased.^{54,63}

The features of the $I_{\text{inc}}(q,t)$ are generally ascribed to a spatial or temporal inhomogeneities in the water diffusion^{54,60} and could be interpreted, in analogy with what was done for supercooled bulk water,^{55,170} in the framework of the MCT.⁶¹ MCT describes the glass transition by taking into account for microscopic density fluctuations in the disordered systems⁶¹ and considers a cage effect associated with a transient trapping of molecules on lowering the temperature or increasing the density. At low temperature, the molecules are trapped in a cage formed by the nearest neighbors.⁶¹ In our case, the water molecule can be rattling in the cage until it reaches a sufficient energy to overcome the energy barrier or to find a vacancy outside the cage.¹⁸⁵ such a hopping process of a single molecule requires a simultaneous rearrangement of a large number of particles surrounding it. In this framework, fast dynamical processes, usually called β relaxations, involve single particle dynamics in the cage formed by the neighboring particles, while the slow ones, or α relaxations, are related to a collective diffusive translation motion beyond the confines of the cage, with fast motions being assumed to be precursor of the slower, collective motions. Such a picture can also provide a ground to interpret the occurrence of anomalous diffusion in the hydration water. Actually, the correlation in the motion of diffusing particles, as connected to escape from the cage, may result into a subdiffusive behavior,^{60,145} and remarkably, it can also provide a consistent scenario to describe the short and the long temporal behavior of protein dynamics.⁵³

3.11. Potential Energy Fluctuations. The temporal evolution of the hydration water potential energy $E_p(t)$ generally reveals fluctuations over a wide range of time scale which may reflect the peculiar features of the dynamics (see, as an example, Figure 11). Information about these fluctuations can be obtained by the power spectra of $E_p(t)$ as calculated by the Fourier transform of the potential energy autocorrelation function:⁷⁰

$$S(f) = \int \langle E_p(0)E_p(t) \rangle e^{2\pi ift} dt \quad (38)$$

Alternatively, the fluctuations in the potential energy can be analyzed by calculating other quantities such as, for instance, the fractal dimension.¹⁸⁶

It has been shown that the power spectrum $S(f)$ of protein hydration water exhibits a power law: $S(f) = 1/f^\alpha$,⁷⁰ the α exponent, generally assuming values around 1 (see upper right inset of Figure 11), may depend on the time interval length used for the analysis.¹⁸⁷ Notably, a $S(f) = 1/f^\alpha$, or flickering, noise, was also detected in the potential energy of bulk water.¹⁸⁸ Generally, the presence of $1/f$ noise, so far observed in a wide variety of different phenomena ranging from physical to biological and social systems, can be hypothesized to be a sort of signature, in the temporal domain, of the complexity of such systems.^{189,190} In particular, the occurrence of $S(f) = 1/f^\alpha$ noise might arise from the existence of multiple time scales.^{79,189} Such a picture finds a correspondence with the power law distribution observed for the residence times of hydration water.¹⁴² However,

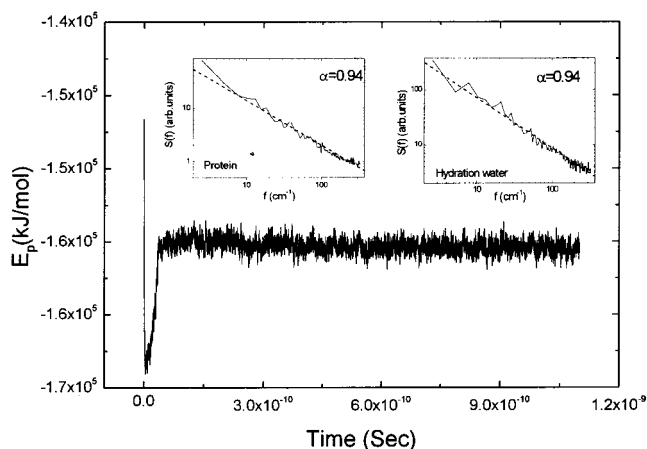


Figure 11. Fluctuations of the total potential energy, at a time resolution of 0.1 ps, along a 0–1100 ps MD trajectory for 3514 SPC/E water molecules around fully hydrated plastocyanin. Upper right inset: power spectrum of the total potential energy for hydration water around plastocyanin. Upper left inset: power spectrum of the total potential energy for the plastocyanin macromolecule. In both the cases, the power spectrum was calculated by eq 38 where the integration was restricted to a time interval corresponding to one-half of the equilibrated trajectory length (500 ps). Dashed line are the best-fit curves of the power spectra by a $1/f^\alpha$ expression; the extracted α values are reported. Adapted from ref 70. The data have been obtained from a MD simulation by GROMOS by using periodic boundary conditions and a cutoff radius of 1.4 nm for the electrostatic interactions.

we remark that the presence of $1/f^\alpha$ noise in the protein hydration water is particularly relevant in connection with the fact that the same feature is observed in the potential energy of a protein macromolecule.⁷⁰ Actually, a $1/f^\alpha$ noise, with the same α exponent detected for the surrounding water, was observed in the potential energy of the plastocyanin (see upper left inset of Figure 11).

Generally, the presence of $1/f^\alpha$ noise can be put into a relationship with the existence in the potential energy landscape of many local minima, separated by unequal barriers, and possibly organized in a hierarchical way, leading to a modulation of the times the system spends in the various states.^{70,72,152} Furthermore, since it was suggested that the $S(f) = 1/f^\alpha$ noise is related to density of states,⁷¹ the possibility that such a phenomenon might be connected to the anomalies observed in the vibrational features in protein systems, e.g., to the boson peak, should be taken into account.

4. Discussion and Future Outlook

Hydration water around a protein macromolecule exhibits dynamical properties markedly deviating from those of bulk. It is of a huge interest to elucidate the mechanisms responsible in determining the peculiar features of the hydration water in the proximity of the protein surface and if these mechanisms could play some role in regulating the protein dynamics and functionality.

The reported overview on the dynamical behavior of the aqueous solvent around globular proteins reveals that the relaxation properties of hydration water significantly deviate from a simple exponential: a stretched exponential providing a well description for the temporal evolution of these quantities. In particular, the relaxation of the survival probability function, of the intermediate scattering function and of the orientational rotational function follow a KWW function: the departure from the exponential decay appearing much more evident as far as water molecules close to the protein surface are taken into

account. Such a relaxation behavior is closely reminiscent of that observed in other disordered, amorphous systems (e.g. in supercooled liquids⁵⁵ and in liquids with a restricted dynamics¹⁹⁰) and it can be interpreted in the framework of MCT.^{60,145} In addition, it is remarkable that water surrounding a protein macromolecule might be an appropriate model to experimentally investigate the glassy behavior of water whose study in the bulk supercooled state can be extremely difficult.¹⁹¹

A further evidence to the glassy character of hydration water comes from the appearance, at low energy, of an excess of vibrational modes, the boson peak: such a vibrational anomaly, whose origin is still under investigation, is generally assumed to be a fingerprint for the amorphous state. In addition, we have seen that the anomalies in the water diffusive properties can be traced back to a disordered state of hydration water, possibly arising from the roughness of the protein SAS, and/or from the peculiar features of protein dynamics.^{60,145}

These results lead to hypothesize that the presence of the biomolecule induces, on the surrounding solvent, a glass-like character, which can strictly mimic the features observed on bulk water by lowering the temperature. A convenient framework for interpreting the topological and dynamical properties of amorphous systems is generally offered by the energy landscape paradigm; such an approach represents a valuable perspective also to describe the dynamics of the protein hydration water. The sampling of the nearly isoenergetic local minima, during the dynamical evolution, strongly dependent on temperature, determines the peculiar dynamical properties of these systems.¹⁹² In particular, it may be responsible for the multiple-time-scale processes which were demonstrated to be at the origin of the stretched exponential decay,¹⁹² and in addition, it could be also invoked to explain the appearance of $1/f^\alpha$ noise, a sort of signature of complexity in the temporal domain.¹⁹³ In this connection, it is rewarding to recall that the protein dynamics shows a glass-like behavior,⁴⁰ e.g., the substrate rebinding kinetics in myoglobin, deviating from an exponential decay, follows a stretched exponential or a power law.³¹ Furthermore, protein dynamics reveals liquid-like features that can be also interpreted in the framework of the MCT.⁵³ In addition, the dynamical transition, connected to the onset of anharmonic motions, at which proteins undergo when the temperature is increased, is reminiscent of a glassy transition.⁴⁰ Accordingly, it was assumed the existence of a huge amount of nearly isoenergetic local minima, called CS, in the energy landscape.²⁶ Such a picture can also provide a framework to interpret other complex aspects appearing in protein systems, e.g., the $1/f^\alpha$ noise,¹⁵² as well as the inhomogeneous broadening observed in the spectral lines detected in many studies on protein samples.^{194–196} Indeed, such an inhomogeneous broadening can be interpreted in terms of a superposition of slightly different signals possibly arising from macromolecules arranged in different CS.^{194–196} On the other hand, the detection of an excess of vibrational modes, at low frequency, in proteins represents a further evidence for their amorphous character.^{67,181} The presence of the boson peak in proteins is particularly intriguing in connection with the simultaneous appearance of a similar spectral feature, and located at the same energy, in the surrounding hydration water. All the above-mentioned observations can be reconciled under the assumption that both the protein and the surrounding aqueous solvent are complex systems, closely similar to glasses, whose energy landscapes are characterized by a multivalley profile with many minima continuously explored during their dynamical evolution. An intriguing open question is represented by the interplay between

the protein and solvent complexity. In particular, we wonder if the glass-like behavior, exhibited by both the protein and the solvent, is a coincidence or it may reflect a deeper coupling, with possible implications for the biological functionality. More generally, a theoretical approach to quantitatively describe the interplay between the protein and the solvent dynamics, should be developed. A complete elucidation of such an interplay, which was subject of many speculations,^{1,2,6,197} may have a substantial impact on the understanding of both the protein and the hydration water.

As it was already remarked, many indications suggest a sort of coupling between the protein and the surrounding solvent dynamics, e.g., the simultaneous appearance, in both the protein and the hydration water, of the boson peak at the same energy, and of $1/f^\alpha$ noise, with the same α exponent. On the other hand, the fact that the solvent-exposed lateral chains of the protein exhibit a relaxation trend similar to that observed in the hydration water, and describable in the same theoretical framework, seems to point toward a strong reciprocal dynamical influence.

A possible viewpoint to interpret the protein–solvent dynamical coupling is represented by the description of a protein system in terms an open Newtonian system (the protein) coupled to a stochastic system (the solvent);¹⁹⁸ the collision between protein and solvent atoms may regulate the diffusion of the biomolecule in the multivalley configuration space of the energy landscape. This finds a correspondence with the picture for which the solvent acts as a plasticizer of the protein motions by injecting its dynamics into the macromolecule possibly through the continuous forming and breaking of hydrogen bonds involving the flexible lateral chains.³³

Alternatively, we can speculate about the possibility that the protein and the solvent should be conceived as a single entity with an unique rough energy landscape. The drastic changes observed in the protein dynamics, as induced by variations in the hydration level, can be seen in terms of the solvent ability to modulate the energy barriers between the protein CS. In other words, we suggest not only that the protein dynamics is “slaved” to the solvent, but the very topological structure of the protein energy landscape could be deeply altered by the spatial organization, as well as by the dynamical behavior of the hydration water.

At the present, it comes out that the protein macromolecule induces a disordered state in the surrounding aqueous solvent that, in turn, is able to control and to regulate the dynamics of the macromolecule itself and, then, the biological functionality. There is a number of interesting open questions related to the protein–solvent interplay, to which MD simulations can give appropriate answers even by performing ad hoc simulated experiments.

A substantial improvement of our knowledge of protein systems should imply a careful analysis of the energy landscapes. In particular, a quantitative description of the energy landscape topography of both the hydration and the macromolecule is required.^{199,200} such an aspect can be of utmost relevance also to elucidate the folding process.¹⁹⁹ Then, according to what recently invoked for glasses,¹⁹² the energy landscape topographic features of the analyzed system are to be directly connected to quantities which can be easily measured. On such a basis, the effects as induced by a modulation of the physico-chemical properties of the surrounding solvent might be clarified.

Other fundamental problems concerning the interplay between the protein and the solvent dynamics, can be afforded by focusing the attention to correlated motions between the protein

and the solvent. In this respect, a suitable tool is represented by the calculation of the spatio-temporal correlations between specific atoms or groups of atoms and water molecules. Such a kind of analysis, whose potentialities are definitely underexploited, might provide useful information to quantitatively elucidate how the solvent dynamics regulates the protein motions. It could also allow ones to investigate the role of fast stochastic solvent motions on the coherent, collective, and macromolecular motions.

Another open question is that related to the contribution to the boson peak from the each protein atom and the interplay on such a vibrational anomaly. In particular, it could be extremely useful to single out the contribution to the boson peak arising from protein atoms characterized by a different exposure to the external solvent. The elucidation of such an aspect could help ones to understand the role played by the solvent in the protein vibrational anomalies as well as in the macromolecular collective motions. At the same time, the analysis of the boson peak in protein systems, allowing ones to focus the attention to the different classes of atoms, could offer the possibility to afford the unresolved aspects about the physical origin of such a peculiar features in amorphous systems.

Finally, the evidence that the macromolecule can deeply affect the water diffusive properties is extremely intriguing in connection with the fact that the surrounding solvent plays a crucial role in many biological processes. The possibility that the anomalous diffusion of hydration water might be related to some mechanisms regulating the biological activity, should be taken into account. For example, it could promote the substrate capture from the bulk, or it could determine a substantial improvement of the exploration of the protein surface from the substrate.^{111,145} In this connection, we can speculate about the possibility that only amino acidic sequences giving rise to particular surface features that are able to yield effective diffusive properties, might be selected by evolution to perform biological functions.

References and Notes

- (1) Gregory, R. B. Ed.; *Protein-Solvent Interactions*; Marcel Dekker, Inc.: New York, 1995.
- (2) Teeter, M. M. *Annu. Rev. Biophys. Biophys. Chem.* **1991**, *20*, 577.
- (3) Poole, P. L.; Finney, J. L. *Biophysics of Water*; Franks, H. S., Ed.; Wiley-Interscience: New York, 1983.
- (4) Singh, G. P.; Parak, F.; Hunklinger, S.; Dransfeld, K. *Phys. Rev. Lett.* **1981**, *47*, 685.
- (5) Koenig, S. H.; Hallenga, K.; Shporer, M. *Proc. Nat. Acad. Sci. U.S.A.* **1975**, *72*, 2667.
- (6) Doster, W.; Bachleitner, A.; Dunau, R.; Hiebl, M. Lüscher, E. *Biophys. J.* **1986**, *50*, 213.
- (7) Otting, G.; Wüthrich, K. *J. Magn. Res.* **1989**, *85*, 586.
- (8) Cheng, S. H.; Schoenborn, B. P. *J. Mol. Biol.* **1991**, *220*, 381.
- (9) Steinhoff, H. J.; Kramm, B.; Hess, G.; Owerdieck, C.; Redhardt, A. *Biophys. J.* **1993**, *65*, 1486.
- (10) Privalov, P. L.; Makhatadze, G. I. *J. Mol. Biol.* **1993**, *232*, 660.
- (11) Denisov, V. P.; Halle, B. *J. Mol. Biol.* **1995**, *245*, 682.
- (12) Denisov, V. P.; Halle, B. *Biochemistry* **1998**, *37*, 9595.
- (13) Middendorf, H. D. *Phys. B* **1996**, *226*, 113.
- (14) Bellissent-Funel, M. C.; Zanotti, J. M.; Chen, S. H. *Faraday Discuss.* **1996**, *103*, 281.
- (15) Halle, B. *Hydration process in Biology: Theoretical and Experimental Approaches*; Bellissent-Funel, M. C., Ed.; IOS Press: Amsterdam, 1999.
- (16) Levitt, M.; Sharon, R. *Proc. Natl. Acad. Sci. U.S.A.* **1988**, *85*, 7557.
- (17) Brunne, R. M.; Liepinsh, E.; Otting, G.; Wüthrich, K.; van Gunsteren, W. F. *J. Mol. Biol.* **1993**, *231*, 1040.
- (18) Phillips, G. N., Jr.; Pettitt, B. M. *Protein Sci.* **1995**, *4*, 149.
- (19) Bizzarri, A. R.; Cannistraro, S. *Phys. Rev. E* **1996**, *53*, 3040.
- (20) Abseher, R.; Schreiber, H.; Steinhauser, O. *Proteins: Struct. Funct. Genet.* **1996**, *25*, 366.
- (21) Kovacs, P.; Mark, A. E.; van Gunsteren, W. F. *Proteins: Struct., Funct., Genet.* **1997**, *27*, 395.
- (22) Denisov, V. P.; Halle, B. *Faraday Discuss.* **1996**, *103*, 227.
- (23) Kuntz, I. D.; Kauzmann, W. *Adv. Protein Chem.* **1974**, *28*, 239.
- (24) Rupley, J. L.; Careri, G. *Adv. Protein Chem.* **1991**, *41*, 37.
- (25) Poole, P. L.; Finney, J. L. *Biopolymers* **1983**, *22*, 255.
- (26) Frauenfelder, H.; Parak, F.; Young, R. D. *Annu. Rev. Biophys. Biophys. Chem.* **1988**, *17*, 451.
- (27) Rasmussen, B. F.; Stock, A. M.; Ringe, D.; Petsko, G. A. *Nature* **1992**, *357*, 423.
- (28) Elber, R.; Karplus, M. *Science* **1987**, *235*, 318.
- (29) Frauenfelder, H.; Sligar, S. G.; Wolynes, P. G. *Science* **1991**, *254*, 1598.
- (30) Angell, C. A. *Science* **1995**, *267*, 1924.
- (31) Ansari, A.; Berendzen, J.; Bowne, S. F.; Frauenfelder, H.; Iben, I. E. T.; Sauke, T. B.; Shyamsunder, E.; Young, R. D. *Proc. Nat. Acad. Sci. USA* **1985**, *82*, 5000.
- (32) Stanley, H. E.; Teixeira, J. *J. Chem. Phys.* **1980**, *73*, 3404.
- (33) Goldanskii, V. I.; Krupyanskii, Y. F. *Quart. Rev. Biophys.* **1989**, *22*, 39.
- (34) Barron, L. D.; Hecht, L.; Wilson, G. *Biochemistry* **1997**, *36*, 13143.
- (35) Green, J. L.; Fan, J.; Angell, C. A. *J. Phys. Chem.* **1994**, *98*, 13780.
- (36) Frauenfelder, H.; Petsko, G. A.; Tsernoglou, D. *Nature* **1979**, *280*, 558.
- (37) Ferrand, M.; Dianoux, A. J.; Petry, W.; Zaccai, G. *Proc. Nat. Acad. Sci. USA* **1993**, *90*, 9668.
- (38) Frick, B.; Richter, D. *Science* **1995**, *267*, 1939.
- (39) Sokolov, A. P. *Science* **1996**, *273*, 1675.
- (40) Iben, I. E. T.; Braunstein, D.; Doster, W.; Frauenfelder, H.; Hong, M. K.; Johnson, J. B.; Luck, S.; Ormos, P.; Schulte, A.; Steinbach, P. J.; Xie, A. H.; Young, R. D. *Phys. Rev. Lett.* **1989**, *62*, 1916.
- (41) Doster, W.; Cusack, S.; Petry, W. *Nature* **1989**, *337*, 754.
- (42) Tilton, R. F.; Dewan, J. C.; Petsko, G. A. *Biochemistry* **1992**, *31*, 2496.
- (43) Parak, F.; Frolov, E. N.; Moessbauer, R. L.; Goldanskii, V. I. *J. Mol. Biol.* **1981**, *145*, 825.
- (44) Karplus, M.; Petsko, G. A. *Nature* **1990**, *347*, 631.
- (45) Smith, J.; Kuczera, K.; Karplus, M. *Proc. Nat. Acad. Sci. U.S.A.* **1990**, *87*, 1601.
- (46) Steinbach, P. J.; Brooks, B. R. *Proc. Nat. Acad. Sci. U.S.A.* **1993**, *90*, 9135.
- (47) Steinbach, P. J.; Brooks, B. R. *Proc. Nat. Acad. Sci. U.S.A.* **1996**, *93*, 55.
- (48) Frauenfelder, H.; Steinbach, P. J.; Young, R. D. *Chem. Scr.* **1989**, *29*, 145.
- (49) Finney, J. L. *Faraday Discuss.* **1996**, *103*, 1.
- (50) Arcangeli, C.; Bizzarri, A. R.; Cannistraro, S. *Chem. Phys. Lett.* **1998**, *291*, 7.
- (51) Vitkup, D.; Ringe, D.; Petsko, G. A.; Karplus, M. *Nat. Struct. Biol.* **2000**, *7*, 34.
- (52) Lee, A. L.; Wand, A. J. *Nature* **2001**, *411*, 501.
- (53) Doster, W.; Cusack, S.; Petry, W. *Phys. Rev. Lett.* **1990**, *65*, 1080.
- (54) Bizzarri, A. R.; Paciaroni, A.; Cannistraro, S. *Phys. Rev. E* **2000**, *62*, 3991.
- (55) Gallo, P.; Sciortino, F.; Tartaglia, F.; Chen, S. H. *Phys. Rev. Lett.* **1996**, *76*, 2730.
- (56) Sartor G.; Mayer, E. *Biophys. J.* **1994**, *67*, 1724.
- (57) Librizzi, F.; Vitrano, E.; Cordone, L. *Biophys. J.* **1999**, *76*, 2727.
- (58) Gekko, K.; Timasheff, S. *Biochemistry* **1981**, *20*, 4677.
- (59) Tsai, A. M.; Neumann, D. A.; Bell, L. N. *Biophys. J.* **2000**, *79*, 2728.
- (60) Settles, M.; Doster, W. *Faraday Discuss.* **1996**, *103*, 269.
- (61) Goetze, W.; Sjoegren, L. *Rep. Prog. Phys.* **1992**, *55*, 241.
- (62) Paciaroni, A.; Bizzarri, A. R.; Cannistraro, S. *Phys. Rev. E* **1998**, *57*, 6277.
- (63) Tarek, M.; Tobias, D. J. *Biophys. J.* **2000**, *79*, 3244.
- (64) Elliott, S. R. *Europhys. Lett.* **1992**, *19*, 201.
- (65) Phillips, W. A. *Amorphous Solids: Low-Temperature Properties*; Springer: Berlin, 1981.
- (66) Cusack, S.; Doster, W. *Biophys. J.* **1990**, *58*, 243.
- (67) Paciaroni, A.; Stroppolo, M. E.; Arcangeli, C.; Bizzarri, A. R.; Desideri, A.; Cannistraro, S. *Eur. Biophys. J.* **1999**, *28*, 447.
- (68) Etchegoin, P. *Phys. Rev. E* **1998**, *58*, 845.
- (69) Paciaroni, A.; Bizzarri, A. R.; Cannistraro, S. *Phys. Rev. E* **1999**, *60*, 2476.
- (70) Bizzarri, A. R.; Cannistraro, S. *Phys. Lett. A* **1997**, *236*, 596.
- (71) Weissman, M. B. *Rev. Mod. Phys.* **1988**, *60*, 537.
- (72) Bizzarri, A. R.; Cannistraro, S. *Phys. A* **1999**, *267*, 257.
- (73) McCammon, J. A. *Rep. Prog. Phys.* **1984**, *47*, 1.
- (74) McCammon, J. A.; Harvey, S. C. *Dynamics of Protein and Nucleic Acids*; Cambridge University Press: Cambridge, 1987.
- (75) Brooks, C. L., III; Karplus, M.; Pettitt, B. M. *Proteins: A Theoretical Perspective of Dynamics Structure and Thermodynamics*; Wiley-Interscience: New York, 1988.
- (76) van Gunsteren, W. F.; Berendsen, H. J. C. *Angew. Chem., Int. Ed. Engl.* **1991**, *29*, 992.

- (77) MacKerrell, A. D., Jr.; Bashford, D.; Bellott, M.; Dunbrack, R. L., Jr.; Evanseck, J. D.; Field, M. J.; Fischer, S.; Gao, J.; Guo, H.; Ha, S.; Joseph-McCarthy, D.; Kuchnir, L.; Kuczera, K.; Lau, F. T. K.; Mattos, C.; Michnick, S.; Ngo, T.; Nguyen, D. T.; Prodhom, B.; Reiher, W. E., III; Roux, B.; Schlenkrich, M.; Smith, J. C.; Stote, R.; Straub, J. M.; Watanabe, M.; Wiorkiewicz-Kuczera, J.; Yin, D.; Karplus, M. *J. Phys. Chem. B* **1998**, *102*, 3586.
- (78) van Gunsteren, W. F.; Berendsen, H. J. C. *Groningen Molecular Simulation (GROMOS) Library Manual*; Biomos: Groningen, 1987.
- (79) Cornell, W. D.; Cieplak, P.; Bayly, C. I.; Gould, I. R.; Merz, K. M., Jr.; Ferguson, D. M.; Spellmeyer, D. C.; Fox, T.; Caldwell, J. W.; Kollman, P. A. *J. Am. Chem. Soc.* **1995**, *117*, 5179.
- (80) Levitt, M.; Hirshberg, M.; Sharon, R.; Daggett, V. *Comput. Phys. Comput.* **1995**, *91*, 215.
- (81) Steinbach, P. J.; Brooks, B. R. *J. Comput. Chem.* **1994**, *15*, 57.
- (82) Barker, L. A.; Watts, R. O. *Mol. Phys.* **1973**, *26*, 789.
- (83) Darden, T.; York, D.; Pedersen, L. *J. Chem. Phys.* **1993**, *98*, 10089.
- (84) Allen, M. P.; Tildesley, D. J. *Computer Simulation of Molecular Liquids*; Clarendon Press: Oxford, 1987.
- (85) Smith, P. E.; Blatt, H. D.; Pettitt, B. M. *J. Phys. Chem. B* **1997**, *101*, 3886.
- (86) Lifson, S.; Oppenheim, I. *J. Chem. Phys.* **1960**, *33*, 109.
- (87) Fraternali, F.; van Gunsteren, W. F. *J. Mol. Biol.* **1996**, *256*, 939.
- (88) Berendsen, H. J. C.; Postma, J. P. M.; van Gunsteren, W. F.; Hermans, J. *Intramolecular Forces*; Pullman, B., Ed.; Reidel: Dordrecht, 1981.
- (89) Berendsen, H. J. C.; Grigera, J. R.; Straatsma, T. P. *J. Phys. Chem.* **1987**, *91*, 6269.
- (90) Jorgensen, W. L.; Chandrasekhar, J.; Madura, J. D.; Impey, R. W.; Klein, M. L. *J. Chem. Phys.* **1983**, *79*, 926.
- (91) Levitt, M.; Hirshberg, M.; Sharon, R.; Laidig, K. E.; Daggett, V. *J. Phys. Chem. B* **1997**, *101*, 5051.
- (92) Stillinger, F. H.; Rahman, A. *J. Chem. Phys.* **1974**, *60*, 1545.
- (93) Jorgensen, W. L.; Tirado-Rives, J. *J. Am. Chem. Soc.* **1988**, *110*, 1657.
- (94) Brooks, C. L., III; Karplus, M. *J. Mol. Biol.* **1989**, *208*, 159.
- (95) Verlet, L. *Phys. Rev.* **1967**, *159*, 98.
- (96) Beeman, D. *J. Comput. Phys.* **1976**, *20*, 130.
- (97) Gear, C. W. *Numerical Initial Value Problems in Ordinary Differential Equations*; Prentice Hall: New York, 1971.
- (98) Ryckaert, J. P.; Ciccotti, G.; Berendsen, H. J. C. *J. Comput. Phys.* **1977**, *23*, 327.
- (99) Andersen, H. C. *J. Chem. Phys.* **1980**, *72*, 2384.
- (100) Berendsen, H. J. C.; Postma, J. P. M.; van Gunsteren, W. F.; Di Nola, A.; Haak, J. R. *J. Chem. Phys.* **1984**, *81*, 3684.
- (101) Hoover, W. G. *Phys. Rev. A* **1985**, *31*, 1695.
- (102) Gerstein, M.; Lynden-Bell, R. M. *J. Mol. Biol.* **1993**, *230*, 641.
- (103) Cantor, C. R.; Schimmel, P. R. *Biophysical Chemistry, Part I*; Freeman and Co.: New York, 1980.
- (104) Lee, B.; Richards, F. M. *J. Mol. Biol.* **1971**, *55*, 379.
- (105) Richards, F. M. *Annu. Rev. Biophys. Bioeng.* **1977**, *6*, 151.
- (106) Chothia, C. *Nature* **1975**, *254*, 304.
- (107) Connolly, M. *Science* **1983**, *221*, 709.
- (108) Einsenberg, F.; Lijnzaad, P.; Argos, P.; Sander, C. Scharf, M. *J. Comput. Chem.* **1995**, *16*, 273.
- (109) Muegge, I.; Knapp, E. W. *J. Phys. Chem.* **1995**, *99*, 1371.
- (110) Hartsough, D. S.; Merz, K. M., Jr. *J. Am. Chem. Soc.* **1993**, *115*, 6529.
- (111) Pfeifer, P.; Welz, U.; Wippermann, H. *Chem. Phys. Lett.* **1985**, *113*, 535.
- (112) Zachmann, C. D.; Kast, S. M.; Sariban, A.; Brickmann, J. *J. Comput. Chem.* **1993**, *14*, 1290.
- (113) Avnir, D.; Ed. *The Fractal Approach to Heterogeneous Chemistry—Surfaces, Colloids, Polymers*; J. Wiley and Sons: New York 1989.
- (114) Ahlström, P.; Teleman, O.; Jönsson, B. *J. Am. Chem. Soc.* **1988**, *110*, 4198.
- (115) Komeiji, Y.; Uebayasi, M.; Someya, J.; Yamato, I. *Proteins: Struct., Funct., Genet.* **1993**, *16*, 268.
- (116) Norin, M.; Haeffner, F.; Hult, K.; Edholm, O. *Biophys. J.* **1994**, *67*, 548.
- (117) Wang, C. X.; Chen, W. Z.; Tran, V.; Douillard, R. *Chem. Phys. Lett.* **1996**, *251*, 268.
- (118) Lounnas, V.; Pettitt, B. M.; Phillips, G. N., Jr. *Biophys. J.* **1994**, *66*, 601.
- (119) Gu, W.; Schoenborn, B. P. *Proteins: Struct., Funct., Genet.* **1995**, *22*, 20.
- (120) Lounnas, V.; Pettitt, B. M. *Proteins: Struct., Funct., Genet.* **1994**, *18*, 133.
- (121) Scanlon, W. J.; Eisenberg, D. *J. Phys. Chem.* **1981**, *85*, 3251.
- (122) Makarov, V. A.; Andrews, B. K.; Smith, P. E.; Pettitt, B. M. *Biophys. J.* **2000**, *79*, 2966.
- (123) Beglov, D.; Roux, B. *Biopolymers* **1994**, *35*, 171.
- (124) Lounnas, V.; Pettitt, B. M. *Proteins: Struct., Funct., Genet.* **1994**, *18*, 148.
- (125) Impey, R. W.; Madden, P. A.; McDonald, I. R. *J. Phys. Chem.* **1983**, *87*, 5071.
- (126) Berendsen, H. J. C.; van Gunsteren, W. F.; Zwinderman, H. R. J.; Geurtsen, R. G. *Ann. New York Acad. Sci.* **1986**, *482*, 268.
- (127) Garcia, A. E.; Stiller, L. *J. Comput. Chem.* **1993**, *14*, 1396.
- (128) Bizzarri, A. R.; Wang, C. X.; Chen, W. Z.; Cannistraro, S. *Chem. Phys.* **1995**, *201*, 463.
- (129) Tirado-Rives, J.; Jorgensen, W. L. *J. Am. Chem. Soc.* **1990**, *112*, 2773.
- (130) Geiger, A.; Stillinger, F. H.; Rahaman, A. *J. Chem. Phys.* **1979**, *70*, 4185.
- (131) Mezei, M.; Beveridge, D. L. *J. Chem. Phys.* **1981**, *74*, 622.
- (132) Stillinger, F. H.; Rahaman, A. *J. Chem. Phys.* **1974**, *60*, 1545.
- (133) Lullzer, A.; Chandler, D. *Nature* **1996**, *379*, 55.
- (134) Finney, J. L.; Gellatly, B. J.; Golton, I. C.; Goodfellow, J. *Biophys. J.* **1980**, *32*, 17.
- (135) Fitter, J. *Biophys. J.* **1999**, *76*, 1034.
- (136) Stillinger, F. H. *Science* **1980**, *209*, 451.
- (137) Wong, C. F.; Zheng, C.; McCammon, J. A. *Chem. Phys. Lett.* **1989**, *154*, 151.
- (138) Reat, V.; Ferrand, M.; Finney, J. L.; Daniel, R. M. Smith, J. C. *Proc. Natl. Acad. Sci. U.S.A.* **2000**, *97*, 9961.
- (139) Demmel, F.; Doster, W.; Petry, W.; Schulte, A. *Eur. Biophys. J.* **1997**, *26*, 327.
- (140) Rocchi, C.; Bizzarri, A. R.; Cannistraro, S. *Chem. Phys.* **1997**, *214*, 261.
- (141) Brugè, F.; Parisi, E.; Fornili, S. L. *Chem. Phys. Lett.* **1996**, *250*, 443.
- (142) Rocchi, C.; Bizzarri, A. R.; Cannistraro, S. *Phys. Rev. E* **1998**, *57*, 3315.
- (143) Garcia, A. E.; Hummer, G. *Proteins: Struct., Funct., Genet.* **2000**, *38*, 261.
- (144) Luise, A.; Falconi, M.; Desideri, A. *Proteins: Struct., Funct., Genet.* **2000**, *39*, 56.
- (145) Bizzarri, A. R.; Rocchi, C.; Cannistraro, S. *Chem. Phys. Lett.* **1996**, *263*, 559.
- (146) Kohlrausch, R. *Ann. Phys. (Leipzig)* **1947**, *12*, 353.
- (147) Blumen, A.; Klafter, J.; Zumofen, G. *Transport and Relaxation in Random Materials*; Klafter, J., Rubin, R. J., Shlesinger, M. F., Eds.; World Scientific: Philadelphia, 1986.
- (148) Phillips, J. C. *Rep. Prog. Phys.* **1996**, *59*, 1133.
- (149) Palmer, R. G.; Stein, D. L.; Abrahams, E.; Anderson, P. W. *Phys. Rev. Lett.* **1984**, *53*, 958.
- (150) Sastry, S.; DeBenedetti, P. G.; Stillinger, F. H. *Nature* **1998**, *393*, 554.
- (151) Stillinger, F. H. *Science* **1995**, *267*, 1935.
- (152) Dewey, T. G.; Bann, J. G. *Biophys. J.* **1992**, *63*, 594.
- (153) Garcia, A. E. *Phys. Rev. Lett.* **1992**, *68*, 2696.
- (154) Kimmich, R.; Gneiting, T.; Kotitschke, K.; Schnur, G. *Biophys. J.* **1990**, *58*, 1183.
- (155) Bellissent-Funel, M. C.; Teixeira, J.; Bradley, K. F.; Chen, S. H.; Crespi, H. L. *Phys. B* **1992**, *180–181*, 740.
- (156) Hertz, H. G. *Ber. Bunsen-Ges. Phys. Chem.* **1971**, *75*, 183.
- (157) McQuarrie, D. A. *Statistical Mechanics*; Harper and Row: New York, 1976.
- (158) Chitra, R.; Yashonath, S. *J. Phys. Chem. B* **1997**, *101*, 5437.
- (159) Alper, H. E.; Bassolino-Klimas, D.; Stouch, T. R. *J. Chem. Phys.* **1993**, *99*, 5547.
- (160) Raghavan, K.; Reddy, M. R.; Berkowitz, M. L. *Langmuir* **1992**, *8*, 233.
- (161) Makarov, V. A.; Feig, M.; Andrews, B. K.; Pettitt, B. M. *Biophys. J.* **1998**, *75*, 150.
- (162) Wong, C. F.; McCammon, J. A. *Isr. J. Chem.* **1986**, *27*, 211.
- (163) Bizzarri, A. R.; Cannistraro, S. *Europhys. Lett.* **1997**, *37*, 201.
- (164) Chiu, S. W.; Clark, M.; Balaji, V.; Subramaniam, S.; Scott, H. L.; Jakobsson, E. *Biophys. J.* **1995**, *69*, 1230.
- (165) Jug, G. *Chem. Phys. Lett.* **1986**, *131*, 94.
- (166) Klafter, J.; Zumofen, G.; Blumen, A. *Chem. Phys.* **1993**, *177*, 821.
- (167) Alexander, S.; Orbach, R. *J. Phys. Lett. (Paris)* **1982**, *43*, 625.
- (168) Saxton, M. J. *Biophys. J.* **1996**, *70*, 1250.
- (169) Zichi, D. A.; Rossky, P. J. *J. Chem. Phys.* **1986**, *84*, 2814.
- (170) Chen, S. H.; Gallo, P.; Sciortino, F.; Tartaglia, F. *Phys. Rev. E* **1997**, *56*, 4231.
- (171) Ediger, M. D.; Angell, C. A.; Nagel, S. R. *J. Phys. Chem.* **1996**, *100*, 13200.
- (172) Smith, J. C. *Q. Rev. Biophys.* **1991**, *24*, 227.
- (173) Kneller, G. R.; Keiner, V.; Kneller, M.; Schiller, M. *Comput. Phys. Comm.* **1995**, *91*, 191.
- (174) Bee, M. *Quasielastic Neutron Scattering: Principles and Applications in Solid-State Chemistry, Biology and Material Science*; Hilger: Bristol, 1988.

- (175) Lovesey, S. *Theory of Neutron Scattering from Condensed Matter*; Oxford Science Publication: Oxford, 1986.
- (176) Venturini, F.; Gallo, P.; Ricci, M. A.; Bizzarri, A. R.; Cannistraro, S. *J. Chem. Phys.* **2001**, *114*, 10010.
- (177) Melchionna, S.; Desideri, A. *Phys. Rev. E* **1999**, *60*, 4664.
- (178) Tarek, M.; Tobias, D. J. *J. Am. Chem. Soc.* **1999**, *121*, 9740.
- (179) Sokolov, A. P.; Kisliuk, A.; Soltwisch, M.; Quitmann, D. *Phys. Rev. Lett.* **1992**, *69*, 1540.
- (180) Painter, P.; Mosher, L.; Rhoads, C. *Biopolymers* **1982**, *21*, 1469.
- (181) Diehl, M.; Doster, W.; Petry, W.; Schober, H. *Biophys. J.* **1997**, *73*, 2726.
- (182) Steinbach, P. J.; Loncharich, R. J.; Brooks, B. R. *Chem. Phys.* **1991**, *158*, 383.
- (183) Angell, C. A.; Poole, P. H.; Shao, J. *Nuovo Cimento* **1994**, *16*, 993.
- (184) Horbach, J.; Kob, W.; Binder, K.; Angell, C. A. *Phys. Rev. E* **1996**, *54*, R5897.
- (185) Kob, W.; Andersen, H. C. *Phys. Rev. E* **1995**, *52*, 4134.
- (186) Lidar, D. A.; Thirumalai, D.; Elber, R.; Gerber, R. B. *Phys. Rev. E* **1999**, *59*, 2231.
- (187) Carlini, P.; Bizzarri, A. R.; Cannistraro, S. *Physica D* **2002**, *165*, 242.
- (188) Ohmine, I. *J. Phys. Chem.* **1995**, *99*, 6767.
- (189) West, B. J.; Shlesinger, M. F. *Int. J. Mod. Phys. B* **1989**, *3*, 795.
- (190) Gallo, P.; Ricci, M. A.; Rovere, M.; Hartnig, C.; Spohr, E. *Europhys. Lett.* **2000**, *49*, 183.
- (191) Peyrard, M. *Phys. Rev. E* **2001**, *64*, 11109.
- (192) Debenedetti, P. G.; Stillinger, F. H. *Nature* **2001**, *410*, 259.
- (193) Bak, P.; Tang, C.; Wiesenfeld, K. *Phys. Rev. Lett.* **1987**, *59*, 381.
- (194) Bizzarri, A. R.; Cannistraro, S. *Eur. Biophys. J.* **1993**, *22*, 259.
- (195) Srajer, V.; Schomachke, K. T.; Champion, P. M. *Phys. Rev. Lett.* **1986**, *57*, 1267.
- (196) Fraga, E.; Webb, M. A.; Kwong, C. M.; Loppnow, G. R. *J. Phys. Chem.* **1996**, *100*, 3278.
- (197) Zanotti, J. M. *Phys. Rev. E* **1999**, *59*, 3084.
- (198) Garcia, A. E.; Blumenfeld, R.; Hummer, G.; Krumhansl, J. A. *Phys. D* **1997**, *107*, 225.
- (199) Czerminski, R.; Elber, R. *Proc. Natl. Acad. Sci. U.S.A.* **1989**, *86*, 6963.
- (200) Ulitsky, A.; Elber, R. *J. Chem. Phys.* **1990**, *92*, 1510.
- (201) Guss, J. M.; Bartunik, H. D.; Freeman, H. C. *Acta Crystallogr. B* **1992**, *48*, 790.